AD-A118 159 NAVAL OCEAN RESEARCH AND DEVELOPMENT ACTIVITY NSTL S--ETC F/G 8/10
STUDIES OF LARGE-SCALE THERMAL VARIABILITY WITH A SYNOPTIC MIXE--ETC(U)
JUN 82 A WARN-VARNAS, M CLANCY, M MORRIS

UNCLASSIFIED NORDA-TN-156 NL

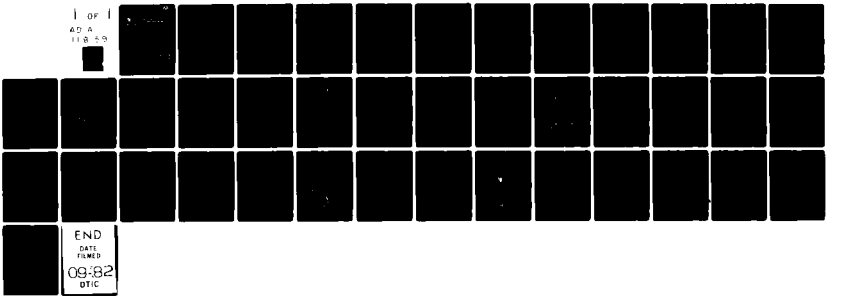

END
DATE FILMED
09-82
DTIC

NORDA Technical Note 156

Naval Ocean Research
and Development Activity
NSTL Station, Mississippi 39529

Studies of Large-Scale Thermal Variability with a Synoptic Mixed-Layer Model

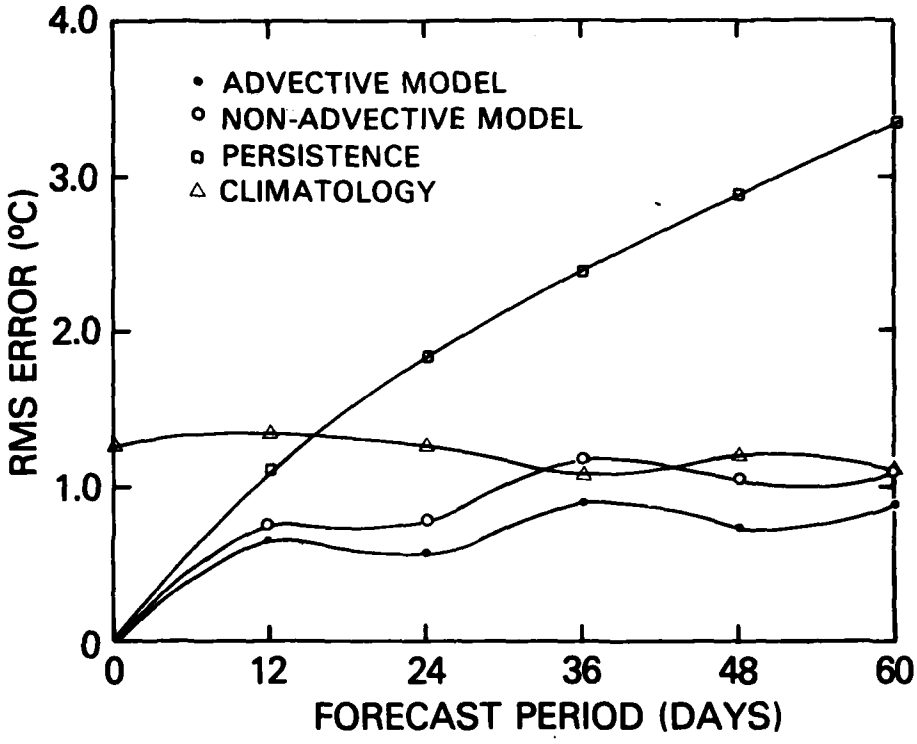

A. Warn-Varnas
M. Clancy
M. Morris
P. Martin
S. Horton

Numerical Modeling Division
Ocean Science and Technology Laboratory

June 1982

ABSTRACT

This work was performed to investigate a number of aspects of operational ocean forecasting including model initialization and forcing, physical parameterizations, and the importance of various processes that modify upper-ocean thermal structure. A synoptic mixed-layer model was used to perform numerical simulations in the TRANSPAC region of the Central North Pacific. The multi-level model incorporates the Mellor and Yamada (1974) Level-2 turbulence parameterization and advection by wind-drift currents.

The model was initialized and forced by fields produced operationally at the U.S. Navy's Fleet Numerical Oceanography Center. Initialization was from the FNOC Ocean Thermal Structure (OTS) analysis and forcing was by surface wind and flux fields associated with the FNOC Northern Hemisphere Primitive Equation and Planetary Boundary Layer Models.

We performed a 60-day simulation of the time span from November to December 1976. Simulations were conducted both with and without wind-drift advection. The results were compared with the daily FNOC OTS analysis, the monthly TRANSPAC XBT analysis, the anomaly calculations of Haney (1980), and forecasts of persistence and climatology.

A comparison of model-predicted sea surface temperature with the OTS analysis showed that the model gave a consistently better forecast than persistence or climatology. Dropping advection from the model decreased its skill. A similar conclusion prevailed when we compared pattern correlations of the predicted and analyzed changes from the initial state.

A comparison of model-simulated changes in upper-ocean heat content with the OTS analysis showed a bias in the FNOC net surface heat flux. The bias was confirmed by a comparison with the flux calculations of Nate Clark. The cause of this bias was most likely excessive latent heat loss.

In the mixed-layer region, the model-simulated anomalies showed a cooling trend in the western two-thirds of the TRANSPAC region and a warming trend in the eastern one-third. This trend agreed with observations. The inclusion of advection improved the agreement.

Variations in initial conditions and analysis of the differences in subsequent solutions showed a propagation of the same difference pattern in time in the mixed layer region. This confirms that upper-ocean variability is dominated by external forcing.

ACKNOWLEDGEMENT

The NORPAX data was supplied by S. Pazan of the Scripps Institution of Oceanography.

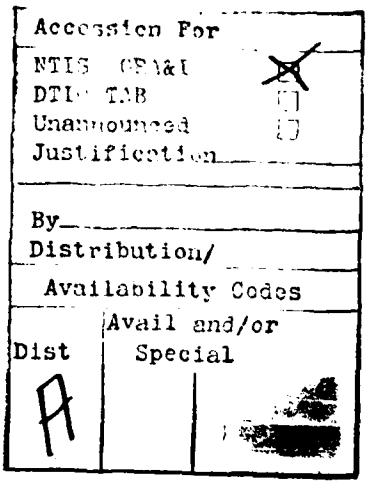

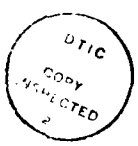

ILLUSTRATIONS

I. INTRODUCTION

In recent years large-scale thermal variability in the Central North Pacific Ocean has been studied by many investigators. Most of the studies were concerned with the explanation of sea surface temperature anomalies. Causes of these anomalies were sought in air-sea heat exchange, atmospherically forced vertical mixing, and advection by geostrophic and wind-driven currents. The contributions of these various mechanisms to the heat budget of the upper ocean were estimated in various ways. Clark (1972) found correlation between the patterns of the observed anomalies and air-sea heat exchange. Camp and Elsberry (1978) simulated upper-ocean response to observed atmospheric forcing with a one-dimensional bulk mixed-layer model, and demonstrated the importance of strong forcing events and vertical mixing processes. Barnett (1981) analyzed AXBT data and found that the seasonal cycle is confined largely to the upper 100 m, and that approximately 90-95% of the variance in the seasonal change of heat storage in the region can be accounted for by air-sea heat exchange and some type of vertical mixing. Barnett also pointed out that there is no agreement on the principal mechanisms responsible for anomaly development. He felt that some of the apparent dichotomies may be due to the importance of different physics in different parts of the ocean.

Haney et al. (1978) and Haney (1980) studied the development of large-scale thermal anomalies in the North Pacific with a three-dimensional numerical model. They found that vertical mixing and horizontal advection of mean temperature by anomalous surface Ekman currents explained a large fraction of the observed temperature anomalies in the upper ocean. The effects of anomalous horizontal advection were confined primarily to the upper 50 meters, while the effects of vertical mixing extended down to 125 m. Anomalous surface heating improved the simulation and was important for the development of a shallow warm anomaly to the east of the large-scale cold anomaly in the Central North Pacific in the fall of 1976. It was found that the temperature anomalies were not simply due to an anomalous initial state.

Our study deals with ocean forecasting from an operational point of view, which involves the predictability of the state of the ocean on the daily to seasonal time scale with numerical models that rely on operational (i.e., real-time) data bases for initial conditions and surface forcing. Our modeling work differs from previous studies in the sense of approach, model used, and sensitivity studies performed.

Our work will focus on predictability and verification studies with various versions of the NORDA Thermodynamic Ocean Prediction System (TOPS) model that is currently used operationally at the U.S. Navy's Fleet Numerical Oceanography Center (FNOC). This model can be described as an "NX1-D" or synoptic mixed-layer model (Clancy et al., 1981). It contains a detailed treatment of thermodynamics and mixed-layer physics, and its primary objective is the prediction of changes in the thermal structure of the upper ocean. For the studies reported here, the model is forced by surface flux fields predicted by FNOC atmospheric models and initialized from the Ocean Thermal Structure (OTS) analysis, which was an operational product at FNOC during the period of interest.

The Central North Pacific during the fall of 1976 was chosen for the present study. This choice was made on the basis of available data associated with the NORPAX experiment and the existence of the previously discussed experimental and modeling work.

Our verification studies involve the comparison of model results with the daily OTS analysis and the monthly NORPAX analysis of the XBT data obtained by the TRANSPAC ships-of-opportunity program (White and Bernstein, 1979). In this way we hope to gain insight into the validity of the model as well as the OTS analysis itself. Comparison with the results of Haney (1980) is also done with an investigation of the effects of model physics, initial conditions, time resolution of forcing, and assumed climatology on the simulated anomalies.

Our statistical studies involve a spectrum of initial conditions obtained by considering a time average and deviation over a chosen time period. The differences in the resulting spectrum of evolving solutions are considered in space and time. Effects on model solutions of variations in atmospheric forcing are also considered.

II. DESCRIPTION OF THE MODEL

A. BASIC EQUATIONS

The basic equations of the model are exactly those of the TOPS model, which is used operationally at FNOC (Clancy et al., 1981; Clancy and Pollak, 1982). They express conservation of temperature, salinity, and momentum in the upper ocean and take the form

$$\frac{\partial \bar{T}}{\partial t} = \frac{\partial}{\partial z}\left(\overline{-w'T'} + \nu\frac{\partial \bar{T}}{\partial z}\right) + \frac{1}{\rho_w c}\frac{\partial \bar{F}}{\partial z}$$
$$- \frac{\partial}{\partial x}(u_a\bar{T}) - \frac{\partial}{\partial y}(v_a\bar{T}) - \frac{\partial}{\partial z}(w_a\bar{T}) + A\left(\frac{\partial^2\bar{T}}{\partial x^2} + \frac{\partial^2\bar{T}}{\partial y^2}\right), \qquad (1)$$

$$\frac{\partial \bar{S}}{\partial t} = \frac{\partial}{\partial z}\left(\overline{-w'S'} + \nu\frac{\partial \bar{S}}{\partial z}\right)$$
$$- \frac{\partial}{\partial x}(u_a\bar{S}) - \frac{\partial}{\partial y}(v_a\bar{S}) - \frac{\partial}{\partial z}(w_a\bar{S}) + A\left(\frac{\partial^2\bar{S}}{\partial x^2} + \frac{\partial^2\bar{S}}{\partial y^2}\right), \qquad (2)$$

$$\frac{\partial \bar{u}}{\partial t} = f\bar{v} + \frac{\partial}{\partial z}\left(\overline{-w'u'} + \nu\frac{\partial \bar{u}}{\partial z}\right) - D\bar{u}, \qquad (3)$$

$$\frac{\partial \bar{v}}{\partial t} = -f\bar{u} + \frac{\partial}{\partial z}\left(\overline{-w'v'} + \nu\frac{\partial \bar{v}}{\partial z}\right) - D\bar{v}, \qquad (4)$$

where T is the temperature, S the salinity, u and v the x- and y-components of the current velocity (the x and y horizontal coordinates are defined relative to the grid), w the z-component of the current velocity, F the downward flux of solar radiation, ρ_w a reference density, c the specific heat of seawater, D a damping coefficient, ν a diffusion coefficient, f the Coriolis parameter, A the horizontal eddy diffusion coefficient, t the time, and z the vertical coordinate (positive upward from the level sea surface). Ensemble means are denoted by ($\bar{}$) and primes indicate departure from these means. The quantities u_a, v_a, and w_a are the x-, y-, and z-components of an advection current, which will be defined in Section 2c.

The advective terms are retained in the temperature and salinity equations and neglected in the momentum equations on the basis of scale analysis (Haney, 1974). Such an analysis shows that the advective terms in the thermal energy equation are of order unity, while the advective terms in the momentum equations are of the order of the Rossby Number. Since the Rossby Number is very small in most regions of the open ocean, the advective terms are dropped in the momentum equations.

Because there are no horizontal pressure gradient terms in (3) and (4), u and v represent the wind-drift component of the current. Neglect of horizontal pressure gradients here is motivated by the fact that geostrophic currents generally do not play an important role in mixed-layer dynamics, which is the issue of most concern in this study.

The terms involving the damping coefficient D in (3) and (4) represent the drag force caused by the radiation stress at the base of the mixed layer associated with the propagation of internal wave energy downward and away from the wind-forced region (e.g., Pollard and Millard, 1970; Niiler and Kraus, 1977). The terms involving ν in Eqs. (1)-(4) account for very weak "background" eddy diffusion (due to intermittent breaking of internal waves, for example) that exists below the mixed layer. We take $D=0.1$ day^{-1} and $\nu = 0.1$ cm^{2}s^{-1} and note that these values are within the range of estimates for these quantities.

The Level-2 turbulence closure theory of Mellor and Yamada (1974) is used to parameterize the vertical eddy fluxes of temperature, salinity, and momentum. This turbulence model has been described in a number of papers (e.g., Mellor and Durbin, 1975; Clancy and Martin, 1981) and will not be presented here. Its energetics are essentially the same as those of Pollard et al. (1973) and Thompson (1976), with the increase in potential energy during mixed-layer deepening due to the buoyancy flux at the layer base balanced locally by mean flow shear generation minus viscous dissipation of turbulent kinetic energy.

The horizontal eddy diffusion coefficient A is simply taken to be equal to a constant value of 10^7cm^{2}s^{-1}, and the divergence of the solar radiation flux is based on the data of Jerlov (1968) for seawater optical type IA.

B. GRID AND FINITE DIFFERENCE SCHEME

A vertically stretched grid of 17 points, extending from the level sea surface to 500 m depth, is used in the model. The quantities $\bar{T}$, $\bar{S}$, $\bar{u}$, $\bar{v}$, u_a and v_a are defined at depths of 2.5, 7.5, 12.5, 17.5, 25, 32.5, 40, 50, 62.5, 75, 100, 125, 150, 200, 300, 400, and 500 m. The vertical eddy fluxes and w_a are defined midway between these depths.

The horizontal grid, on which $\bar{T}$, $\bar{S}$, $\bar{u}$, $\bar{v}$, and w_a are defined, is a rectangular subset of the standard FNOC 63 x 63 Northern Hemisphere Polar Stereographic Grid,

and is shown in Figure 1. The mesh spacing at midlatitudes is roughly 300 km. The horizontal components of the advection current are defined on a staggered grid, with u_a and v_a displaced one-half gridlength in the x- and y-directions, respectively, from the grid of Figure 1.

The vertical eddy flux terms in Eqs. (1)-(4) are differenced backward in time. The Coriolis and vertical advection terms are differenced trapezoidal in time, and all other terms are differenced forward in time. All spatial derivatives are centered in space. See Clancy (1981) for an analysis of the numerical stability of the advective terms.

C. CALCULATION OF THE ADVECTION CURRENT

The current used to advect the temperature and salinity is given by

$$u_a = u_i + u_g^* ,$$
$$v_a = v_i + v_g^* , \qquad (5)$$
$$w_a = w_i ,$$

where u_i and v_i are the x- and y-components of the instantaneous wind-drift current, w_i is the vertical component of the current resulting from the divergence of u_i and v_i, and u_g^* and v_g^* are the components of a divergence-free geostrophic current. The geostrophic current is set to zero for all calculations presented here.

D. INITIAL CONDITIONS

The initial temperature for the model is provided by fields produced by the FNOC OTS Analysis System. The OTS analysis is based on the Fields-by-Information-Blending methodology (Holl and Mendenhall, 1971) and was used at FNOC in the mid-1970's to produce daily objective analyses of ocean thermal structure in the upper 400 m. It utilized the FNOC Northern Hemisphere grid (see Fig. 1) and had approximately 25 m vertical resolution in the upper 100 m.

The data input to the analysis consisted of all available real-time XBT and ship injection/bucket temperature observations. Since information was blended vertically as well as horizontally by OTS, the sea surface temperature observations contributed information to the subsurface thermal analysis (Holl et al., 1979). In the absence of nearby data, the analyzed temperatures relaxed toward climatology with an e-folding time scale of about one month (Weigle and Mendenhall, 1974).

Since salinity observations are not routinely made, a synoptic analysis of salinity is not available. Consequently, the initial salinity for the model forecasts is given by climatology, with a slight adjustment from climatology applied in the mixed layer to make the initial density stratification neutral there.

The initial momentum field is set to zero below the mixed-layer base. In the mixed layer, it is taken to vary linearly from a value of zero at the mixed-layer base to a value at the surface chosen so that the mixed-layer-averaged flow is equal to the steady solution of the vertical averages of Eqs. (3) and (4), with the eddy fluxes of momentum given by the initial wind stress at the sea surface and set to zero at the layer base.

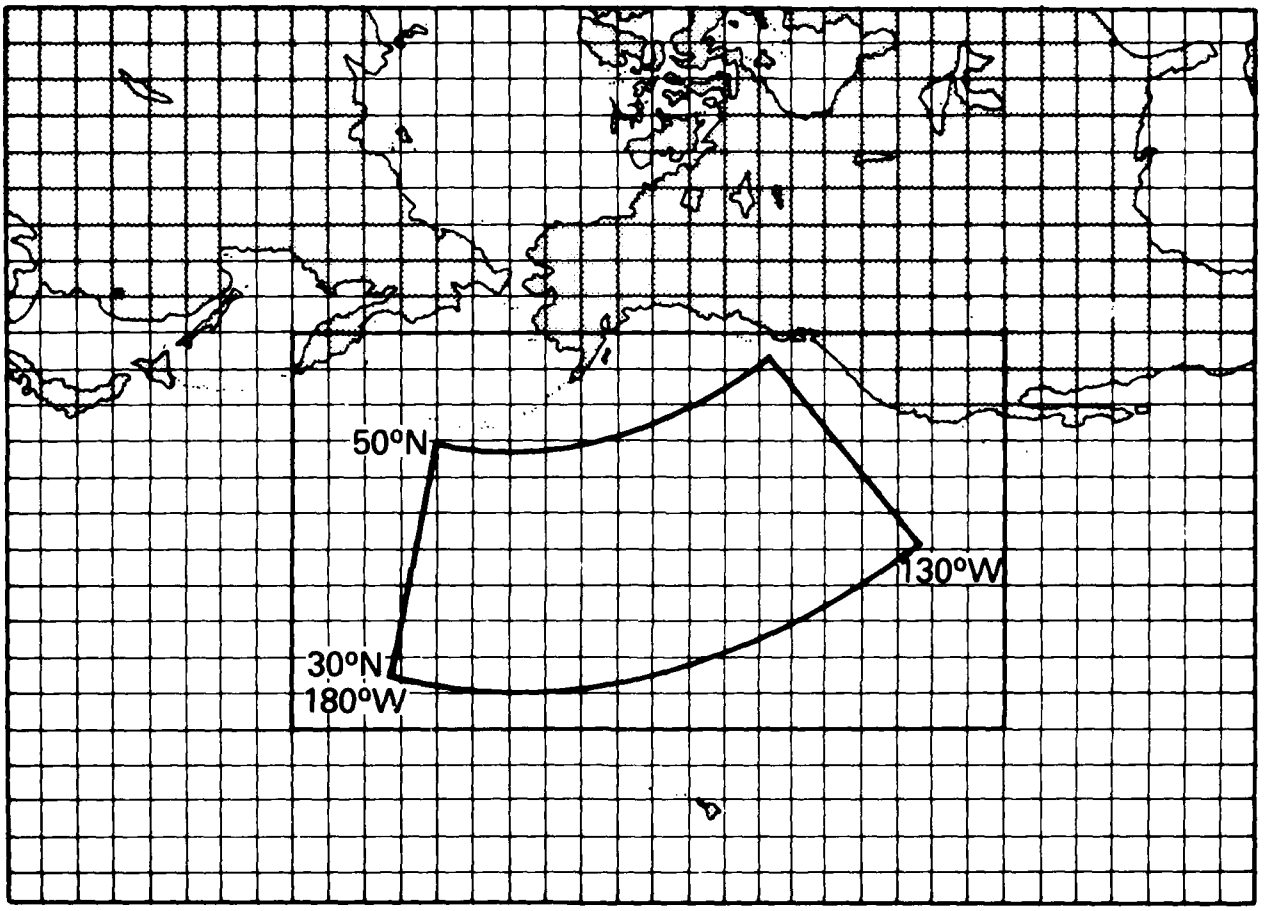

Figure 1. Subsection of the FNOC 63x63 Northern Hemisphere Polar Stereographic Grid showing the model domain (rectangle) and the TRANSPAC region (subarea inside rectangle).

E. BOUNDARY CONDITIONS

The lower boundary conditions for the basic equations are provided by simply holding the initial temperature, salinity, and momentum at the lower boundary of the model constant throughout the integration. The upper boundary conditions are supplied by surface fluxes of heat, moisture, and momentum. Thus,

$$\left[\overline{-w'T'} + \nu\frac{\partial\bar{T}}{\partial z}\right]_{z=0} = \frac{-(B_o + H_o + LQ_o)}{\rho_w c}, \tag{6}$$

$$\left[\overline{-w'S'} + \nu\frac{\partial\bar{S}}{\partial z}\right]_{z=0} = \frac{(Q_o - P_o)\bar{S}_o}{\rho_w}, \tag{7}$$

$$\left[\overline{-w'u'} + \nu\frac{\partial\bar{u}}{\partial z}\right]_{z=0} = \frac{\tau^x}{\rho_w}, \tag{8}$$

$$\left[\overline{-w'v'} + \nu\frac{\partial\bar{v}}{\partial z}\right]_{z=0} = \frac{\tau^y}{\rho_w}, \tag{9}$$

where B_o is the surface infrared radiative heat flux, H_o is the surface sensible heat flux, LQ_o is the surface latent heat flux, P_o is the surface precipitation rate, S_o is the surface salinity, and τ^x and τ^y are the components of the surface wind stress, calculated from

$$\tau^x = \rho_a C_D U(U^2 + V^2)^{1/2}, \tag{10}$$

$$\tau^y = \rho_a C_D V(U^2 + V^2)^{1/2}. \tag{11}$$

Here U and V are the x- and y-components of the wind velocity vector at a reference level of 19.5 m above the sea surface, ρ_a is a reference density for air, and C_D is a constant drag coefficient of 1×10^{-3}.

The quantities U, V, $(B_0 + H_0 + LQ_0)$, Q_0 and P_0 are obtained at 12-hour intervals on the grid of Figure 1 from archived FNOC fields, which are based on analyses and predictions associated with the FNOC Northern Hemisphere Primitive Equation and Planetary Boundary Layer Models (see Kesel and Winninghoff, 1972; Mihok and Kaitala, 1976). They are interpolated to each time step of the model from the 12-hourly values using a cubic interpolation scheme. A surface solar radiative heat flux F_0 is also required to provide an upper boundary condition for the radiational heating calculations. It is determined each time step from

$$F_0 = I_0 \cos \alpha (0.7)^{\sec \alpha} \tag{12}$$

where I_0 is the amplitude of the solar flux and α is the instantaneous zenith angle of the sun. An instantaneous surface solar flux, predicted daily for 0000 GMT by the FNOC PE model (Mihok and Kaitala, 1976), is used to estimate I_0 daily at each model gridpoint from

$$I_0 = \frac{F_1}{\cos \alpha_1 \, (0.7)^{\sec \alpha_1}} \tag{13}$$

where F_1 is the instantaneous flux and α_1 is the instantaneous solar zenith angle associated with F_1. If α_1 is greater than about 75°, however, I_0 cannot be reliably estimated from Eq. (13). In this situation, which occurs at a few gridpoints in the high latitudes during winter, I_0 is simply assumed to be one-half the solar constant.

At both the open and closed (i.e., land-sea) lateral boundaries of the model (see Fig. 1), the normal components of the advection current and the normal derivatives of temperature and salinity are taken to be zero. Thus, no advection or diffusion of temperature or salinity into or out of the model domain is permitted.

III. STUDIES AND DISCUSSION

The region of study, located in the Central North Pacific Ocean from 30°N to 50°N and 130°W to 180°W, will be referred to as the TRANSPAC region. The period of study is fall 1976. The model described in Section 2 is initialized at 0000 GMT 29 October 1976 from the OTS analysis and forced for 60 days by the FNOC latent and sensible heat fluxes, back radiation, solar radiation, precipitation, evaporation, and wind stress.

Our studies of the resulting model predictions are roughly divided into heat content calculations, comparisons with the OTS and NORPAX ocean thermal analyses, and variations in initial conditions and atmospheric forcing.

A. HEAT CONTENT CALCULATIONS

One of the first problems that became evident was a bias in the FNOC net surface heat flux. Problems with the FNOC heat fluxes in the TRANSPAC region have been noted previously by Elsberry et al. (1979) and Budd (1980). They examined the accuracy of the FNOC heat fluxes through a comparison with the observed upper ocean heat content changes derived from the TRANSPAC XBT data. We pursued the problem by performing several studies. In one study we compared the monthly averaged FNOC net heat flux against the monthly averaged NORPAX heat fluxes calculated by N. Clark (private

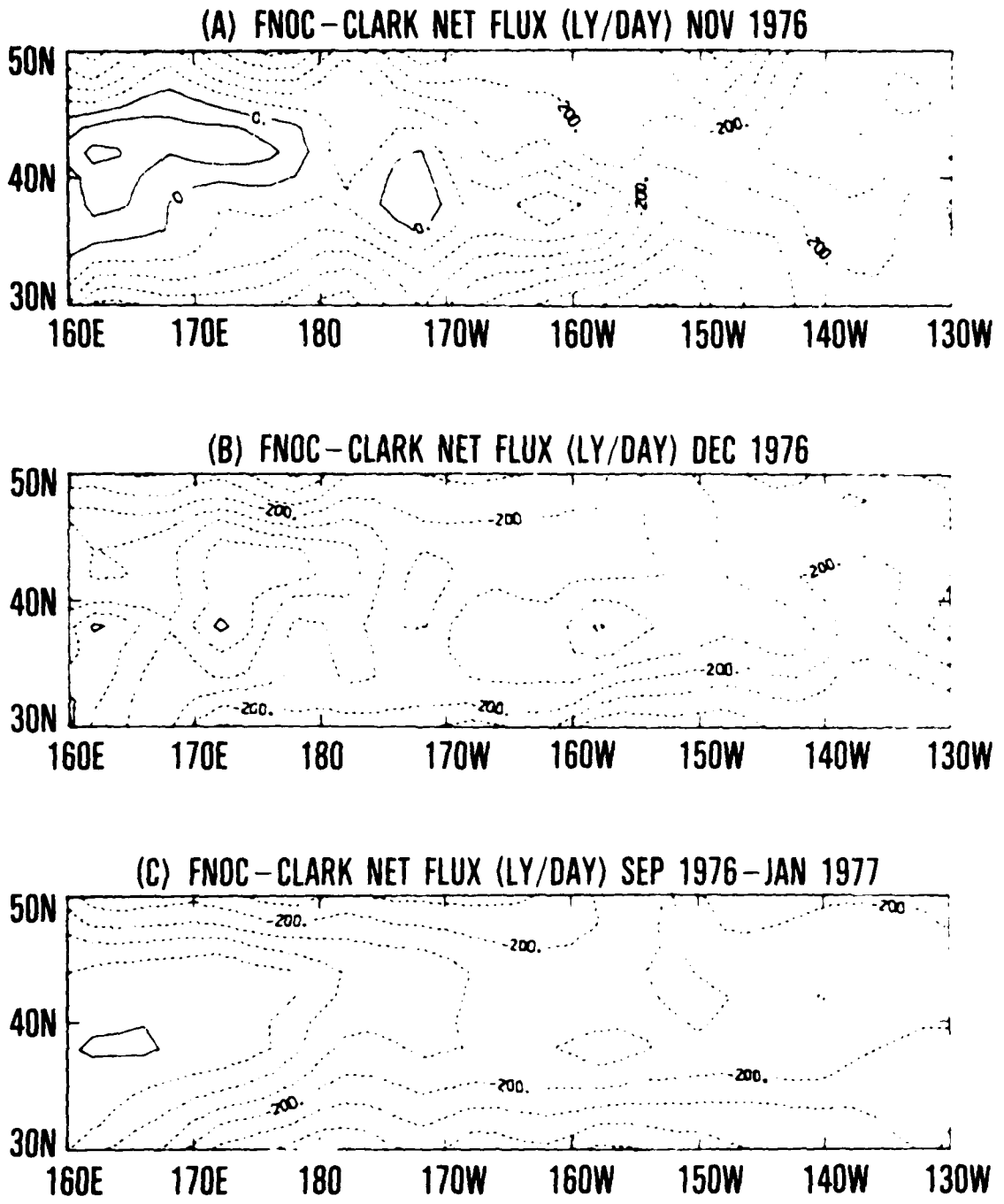

Figure 2. FNOC net surface heat flux minus NORPAX net surface heat flux averaged for (A) November 1976, (B) December 1976, and (C) September 1976 through January 1977. NORPAX heat flux courtesy of N. Clark.

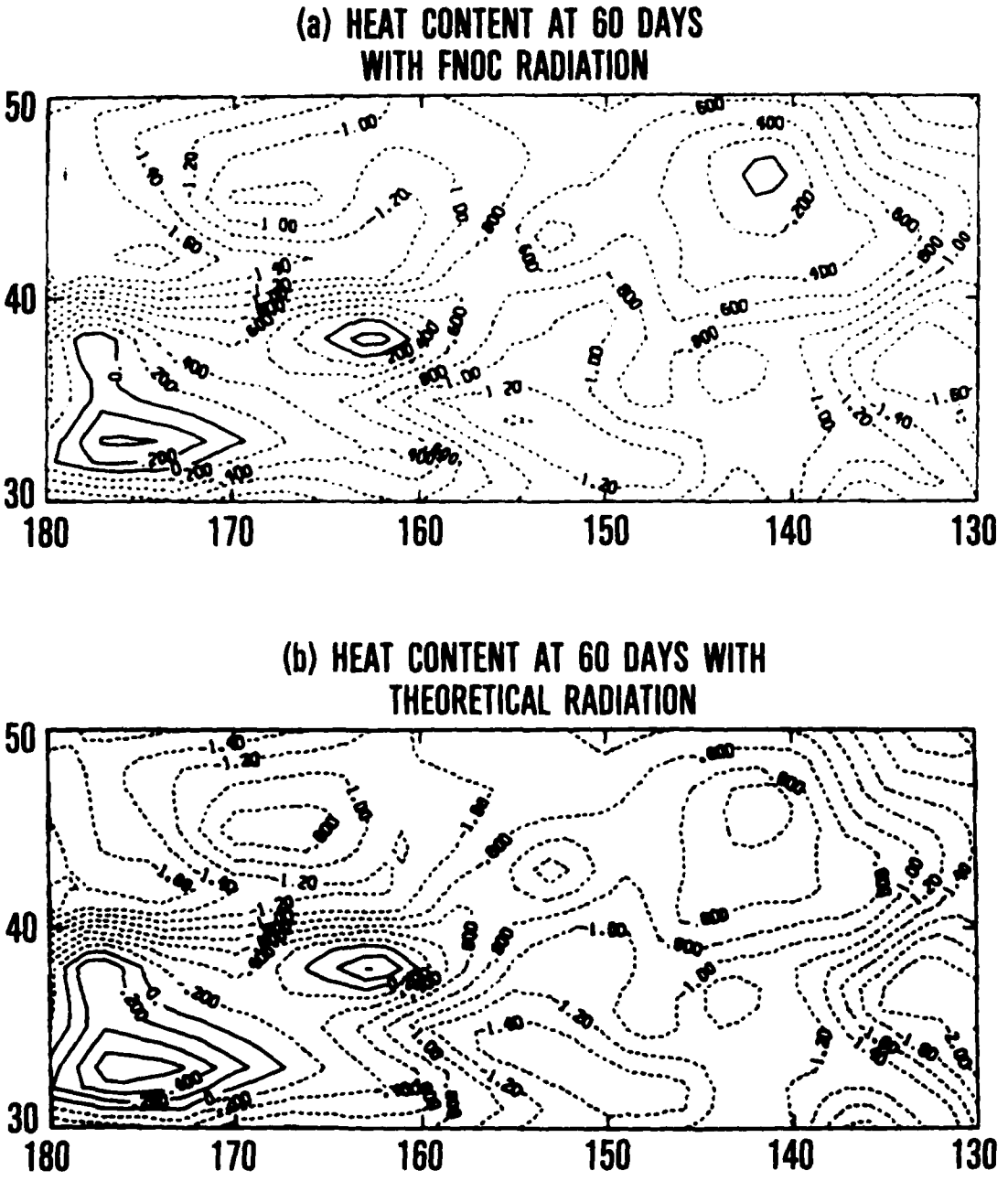

Figure 3. Contours of heat content in the upper 100 m for two different treatments of solar radiation.

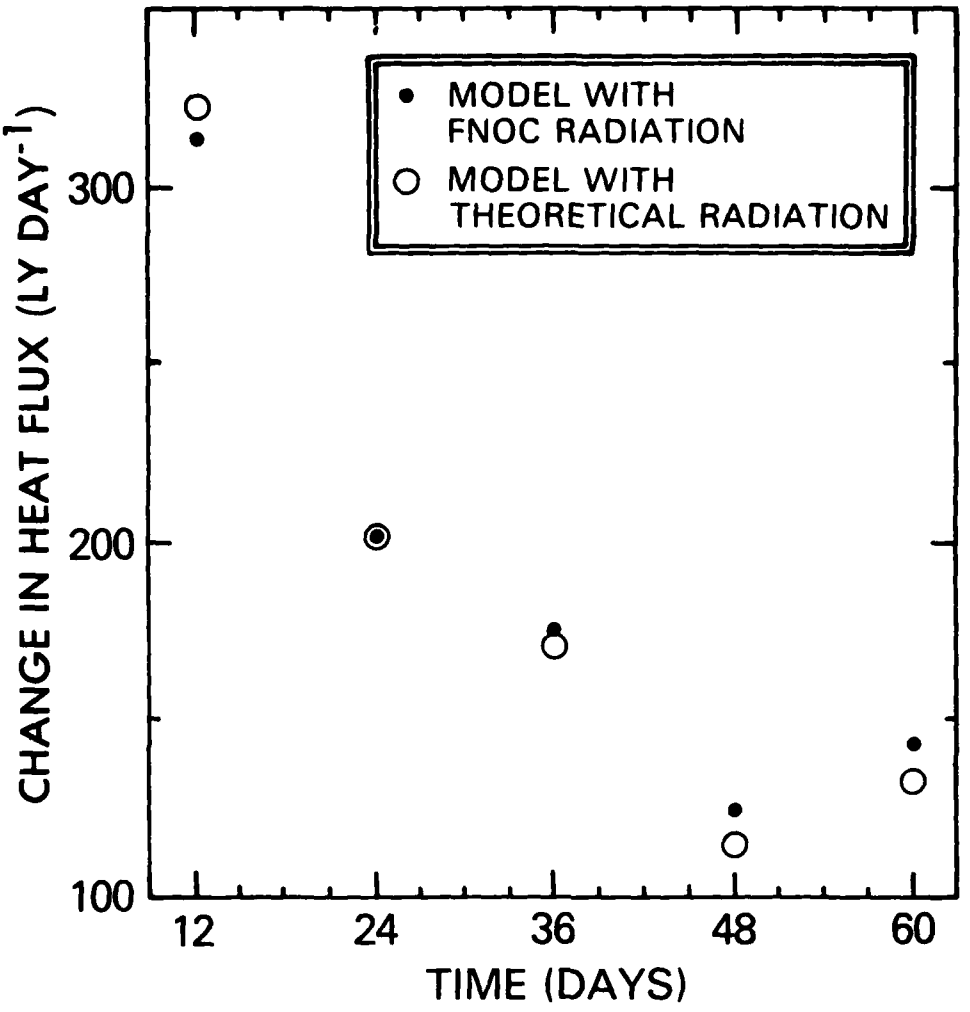

Figure 4. Difference between model and OTS heat content change over the previous twelve-day interval for the TRANSPAC region as a function of forecast time. The results are expressed in the form of an equivalent change in the average net surface heat flux (positive downward) required to make the model heat content change equal to the OTS heat content change over the twelve-day interval. Heat contents are integrated over the upper 100 m.

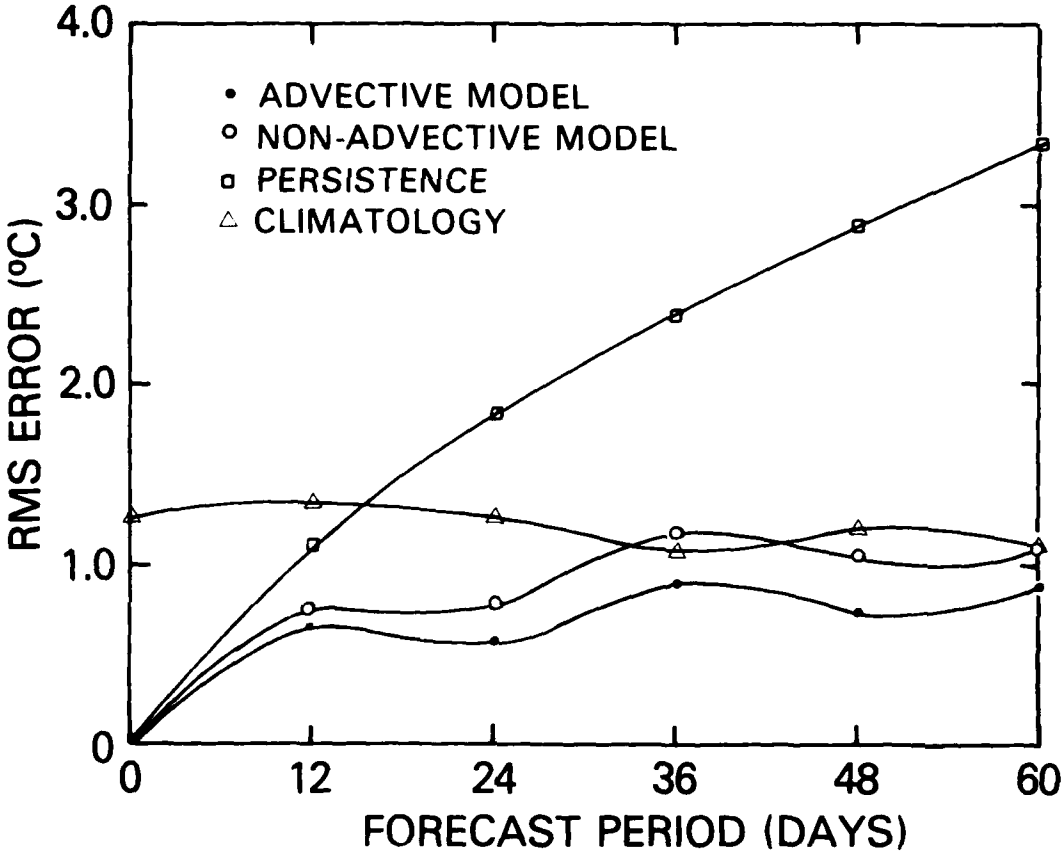

Figure 5. RMS SST forecast errors for the TRANSPAC region as a function of forecast time. The OTS analysis was used for verification.

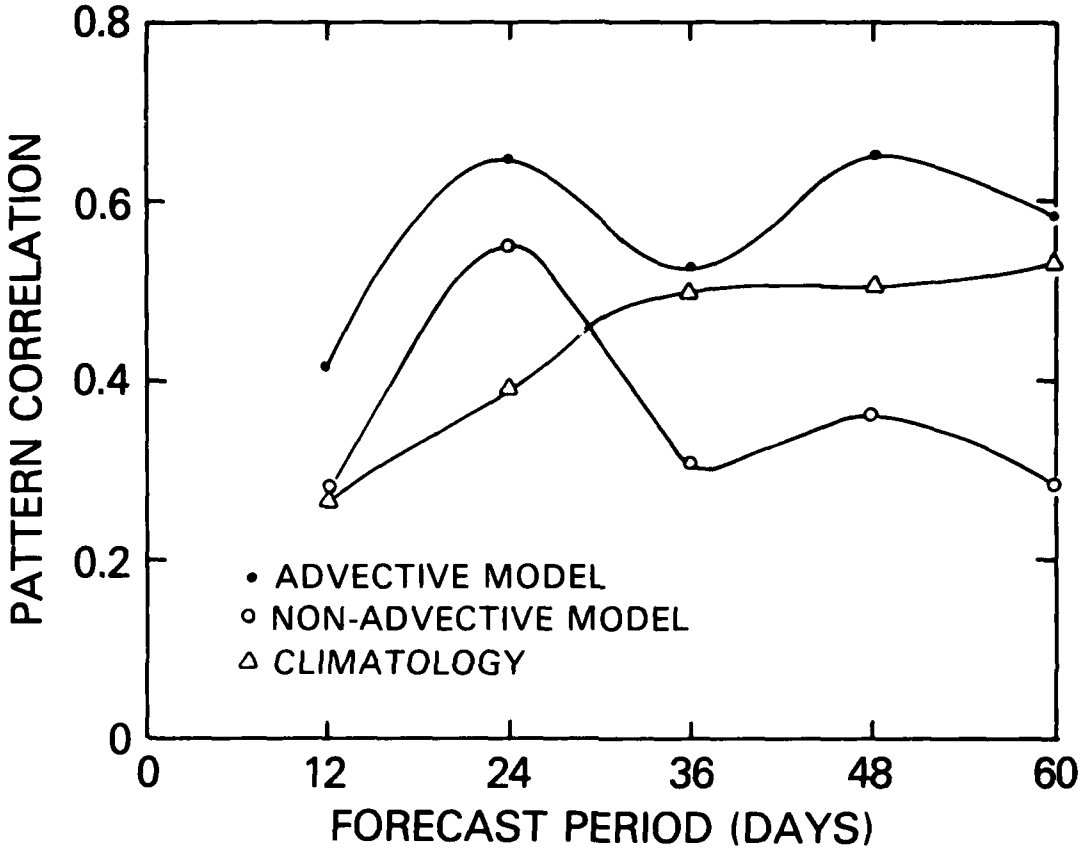

Figure 6. Pattern correlations between forecast and analyzed changes in SST from the initial state. The OTS analysis provided the analyzed changes.

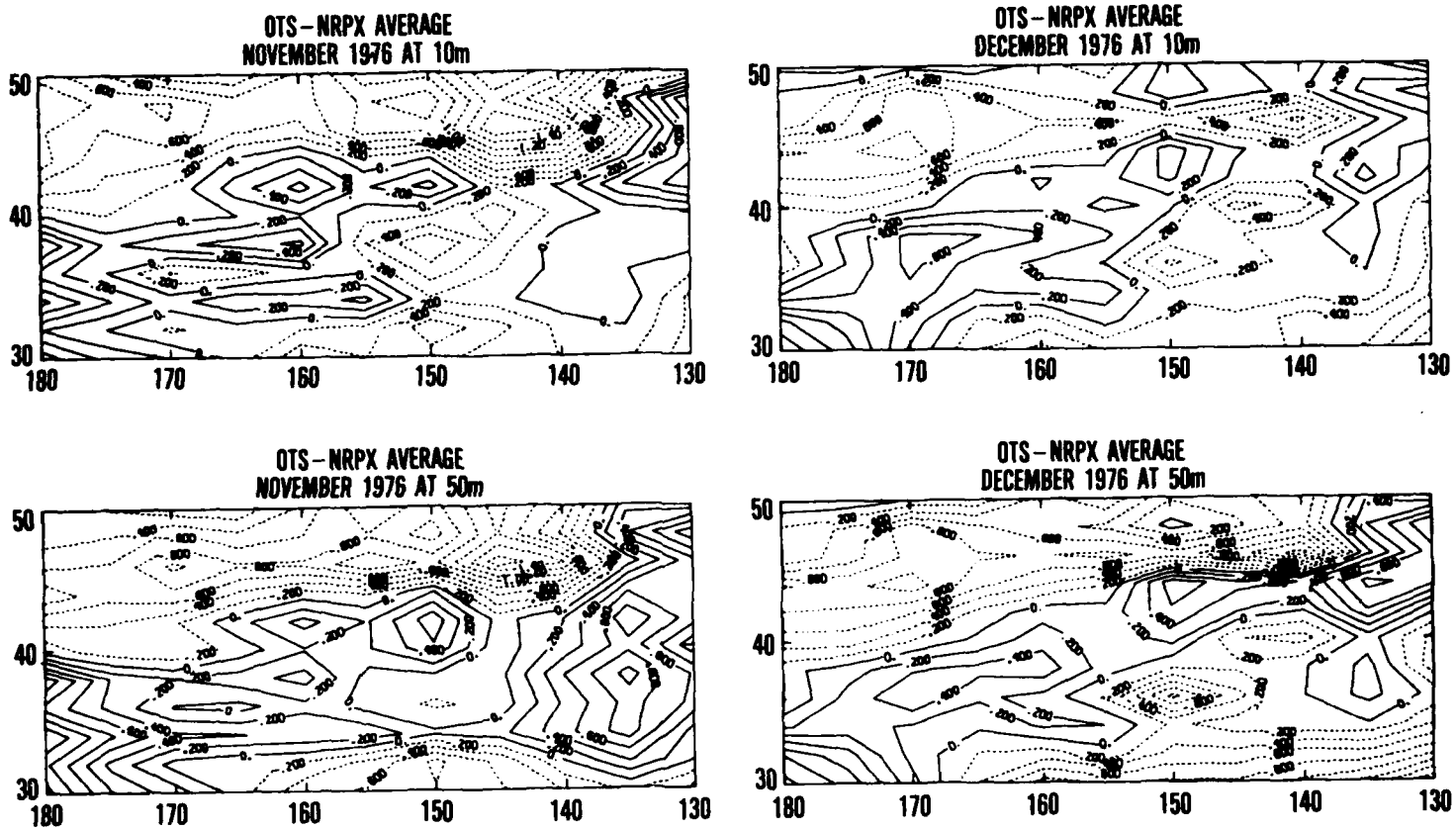

Figure 7a. Differences, in °C, between the monthly averaged OTS analysis and the monthly averaged NORPAX analysis.

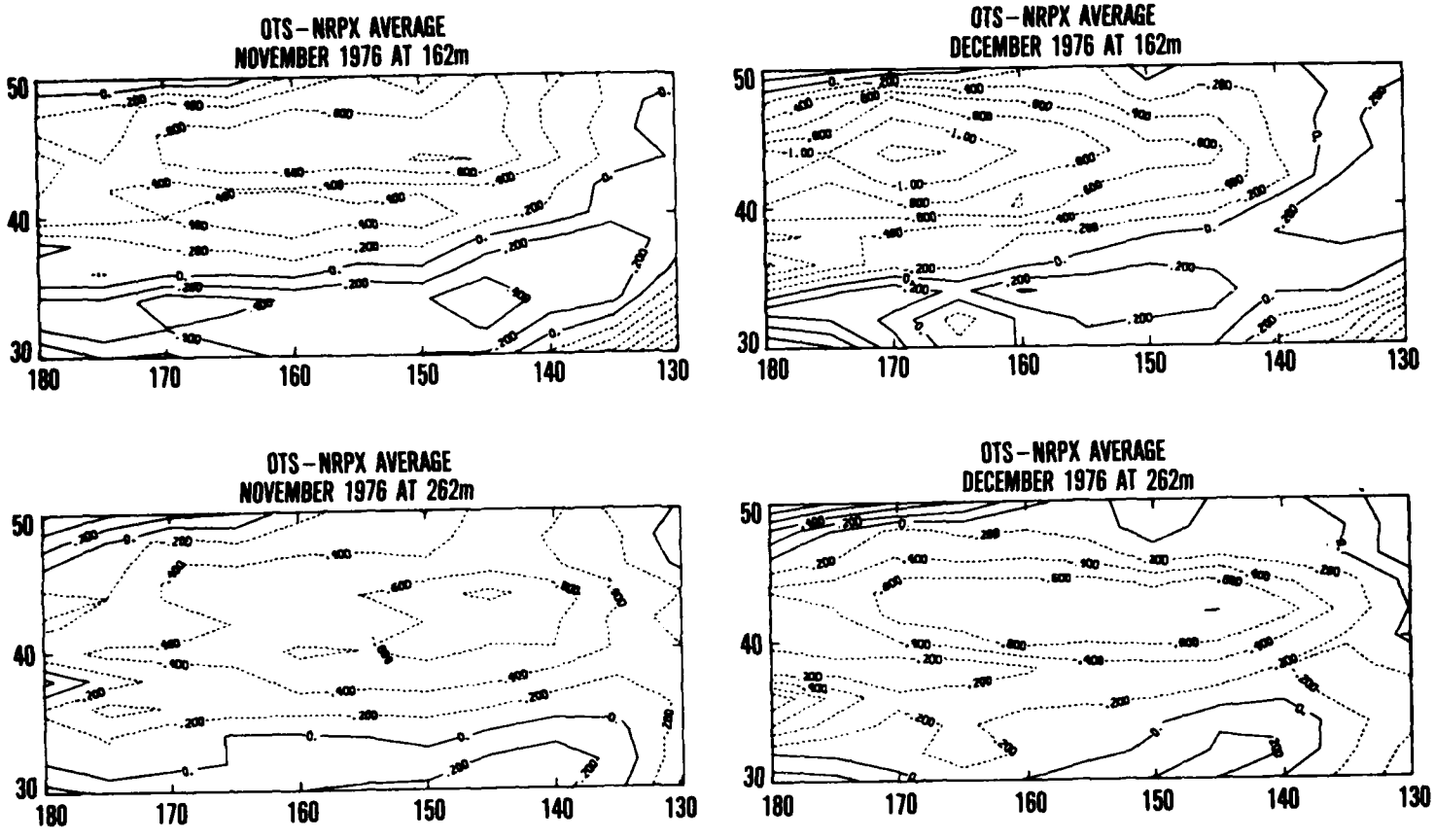

Figure 7b. Differences, in °C, between the monthly averaged OTS analysis and the monthly averaged NORPAX analysis.

communication). Some of the results are shown in Figure 2. The monthly averaged difference of the net heat fluxes over the TRANSPAC region varied from 140 ly day^{-1} to 240 ly day^{-1} from September 1976 to January 1977. This yielded an average cooling of 169 ly day^{-1} for the FNOC fluxes relative to the Clark results.

In addition, we investigated the correctness of the FNOC solar radiation by replacing it with a theoretical formula. This theoretical formula, used by Haney et al. (1978), is

$$F_0 = .95(.74 - .6\,\eta)S_A^*$$

where S_A^* is the flux of solar radiation at the top of the atmosphere, and η is the fractional cloud cover. The quantity η was calculated by interpolation from climatological cloud cover data.

We calculated the heat content, $Q = \rho_0 c \int T dz$, of the upper ocean for both the FNOC and theoretical treatments of the solar radiation. We chose an integration depth of 100 m since that was below the deepest mixed-layer depths observed during the numerical simulation. The results at the end of 60 days are shown in Figure 3. Both formulations gave similar results. The differences can be attributed to the use of climatological cloud cover in the theoretical formula.

The differences in heat content changes between model results and OTS analysis were also computed for both radiation formulations. The results at 12-day intervals are shown in Figure 4. Again, the two treatments gave similar results. On this basis, we concluded that the FNOC solar radiation was approximately correct. Consequently, the excess cooling of the model simulation relative to the OTS analysis was attributed to a bias in one of the other components of the FNOC net heat flux. If we assume that the back radiation is correct, then the problem is most likely in the latent heat flux since the sensible heat flux is too small to account for the error.

Subsequently, we tried two alternative corrections to the FNOC net surface heat flux. One correction used was the averaged, spatially dependent adjustment shown in Figure 2 for the months of September through January. The other correction was simply a reduction in the surface cooling of 150 ly day^{-1} at all points, obtained from an average of the results shown in Figure 4.

B. VERIFICATION STUDIES

Verification studies were performed by comparing model, persistence, and climatological forecasts with the OTS analysis. The OTS analysis, in turn, was monthly averaged and compared with the monthly averaged NORPAX XBT analysis.

Figure 5 shows root-mean-square (RMS) sea surface temperature (SST) forecast errors for the TRANSPAC region produced by persistence, climatology, the model with wind-drift advection, and the model without advection for a case in which the surface heat flux was corrected by a constant 150 ly day^{-1}. The RMS errors are defined relative to the daily OTS analysis. The persistence forecast, defined as a forecast of no change from the initial state, shows the largest RMS error, indicating that the ocean changes significantly from the initial state as time goes by. The figure also shows that the advective version of the model gives a smaller RMS error than the non-advective version (i.e., one which neglects all terms involving u_a, v_a, w_a and A in Eqs. (1)-(4)). The climatological and non-advective model curves cross occasionally in time, indicating a comparable RMS error for these forecasts.

However, it must be remembered that the OTS analysis against which we are comparing relies heavily on climatology (Mendenhall et al., 1978). This generates a bias towards climatology in data-sparse regions, which may tend to make the climatology forecast appear better than is justified.

Relative to persistence, the model exhibited skill in forecasting the temperature change over a period of 60 days. The advective model's RMS error was about a quarter of the persistence error at 60 days. Thus the model could be used to represent the state of the ocean for regions where the ocean thermal data is sparse.

In Figure 6 we show pattern correlations between forecast and analyzed changes in SST from the initial state. Again, the advective version of the model gave the best results. Furthermore, the climatological forecast produced a higher correlation than the nonadvective version of the model. This suggests that there is a signature of the advective effects in the OTS analysis. With regard to the correlation between climatology and the OTS analysis, we again suspect that the results may appear better than is justified because of the bias of OTS towards climatology.

It was also of interest to compare the OTS analysis against the monthly averaged NORPAX analysis. We made such a comparison in Figure 7 by monthly averaging the OTS analysis and subtracting the NORPAX analysis. As indicated by the figure, this difference in temperature on the monthly time scale is approximately ±1°C. A comparison of the difference patterns at 2.5 m (not shown in Fig. 7), 10 m, and 50 m shows a weak correlation between these depths. This upper region of about 50 m roughly defines the mixed layer. As we go deeper, to depths of 162 m and 262 m, the structure of the difference patterns becomes simpler, and there is an overall tendency for the OTS analysis to give lower temperatures than the NORPAX analysis. In the upper region, there is a tendency for the OTS analysis to be colder than the NORPAX analysis in the northwestern quadrant and warmer in the southwestern quadrant. In the far northeastern quadrant, the OTS analysis is warmer.

At this point we return to the model results for a more detailed comparison with the OTS analysis. In Figure 8, we show one such comparison of the difference between model prediction with wind-drift advection, and the OTS analysis. The correction to the net heat flux was 150 ly day^{-1}. The differences at each point are averaged in time over 12-day intervals. At the 2.5 m level, the point of reference for SST, we observe certain trends. The magnitude of the differences is plus or minus one degree. In the far eastern and northwestern regions the model results are colder than the OTS analysis. There is a tendency for coherence of the difference patterns in the upper region. At a 102 m there is an average tendency for the model results to be colder than the OTS analysis.

C. ANOMALY CALCULATIONS AND STUDIES

Another study performed was the calculation of temperature anomalies (i.e., deviations from climatology) from the model predictions. These anomalies were compared with the monthly averaged anomalies calculated from the NORPAX analysis. The development of these anomalies can be characterized by the formation of an intensely cold anomaly in the upper 100 m over the western two-thirds of the region and the formation of a shallow warm anomaly in the eastern third of the region. In all cases, the anomalies are defined relative to the NORPAX climatology.

The initial anomalies are shown in Figure 9. The pattern correlation between the model-predicted SST anomalies and anomalies calculated from the OTS analysis are shown in Figure 10. The correlations are generally high, indicating that the

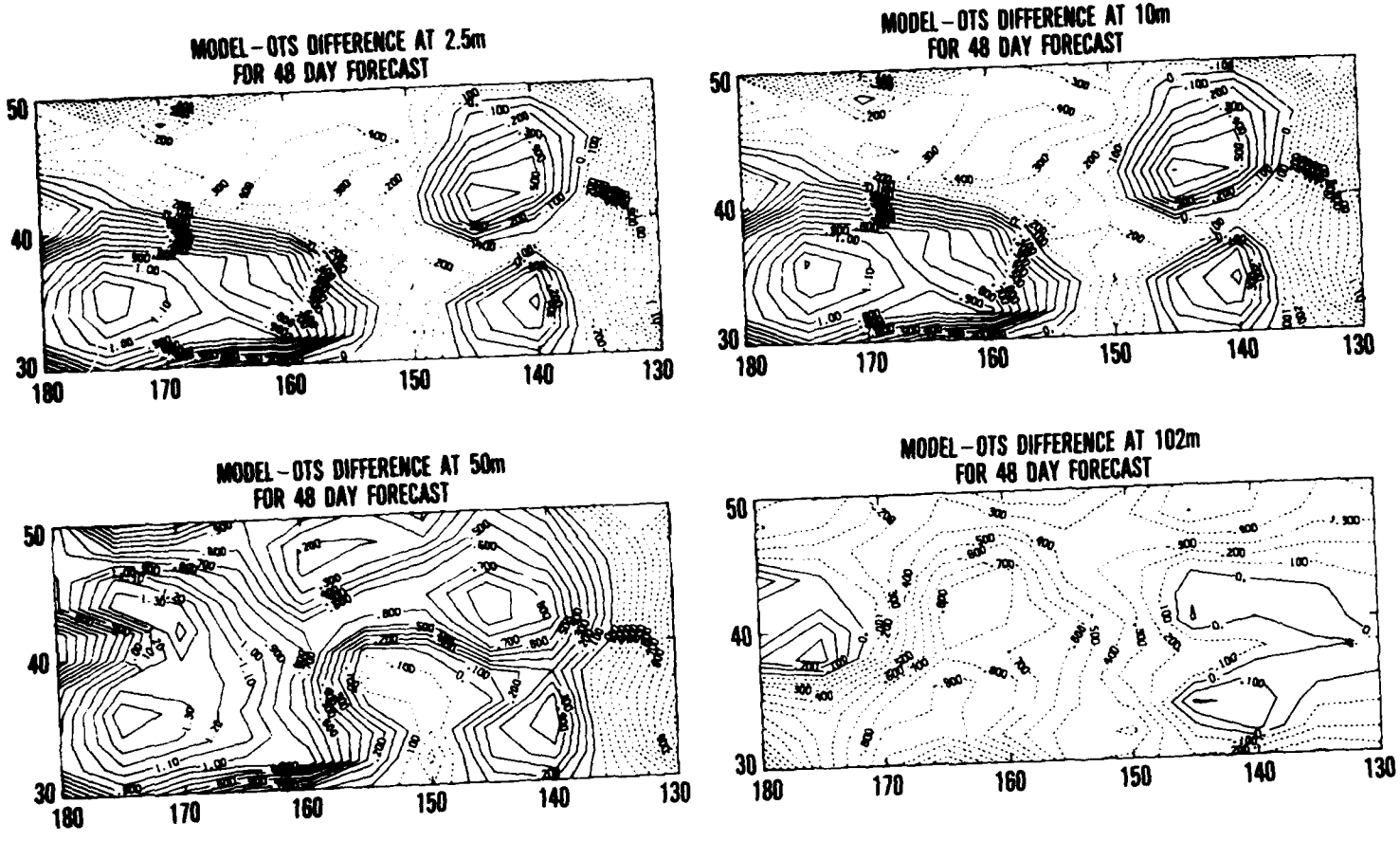

Figure 8. Differences between the model simulations and the OTS analysis. Each result is averaged over a twelve-day interval centered at Day 48. The units are °C.

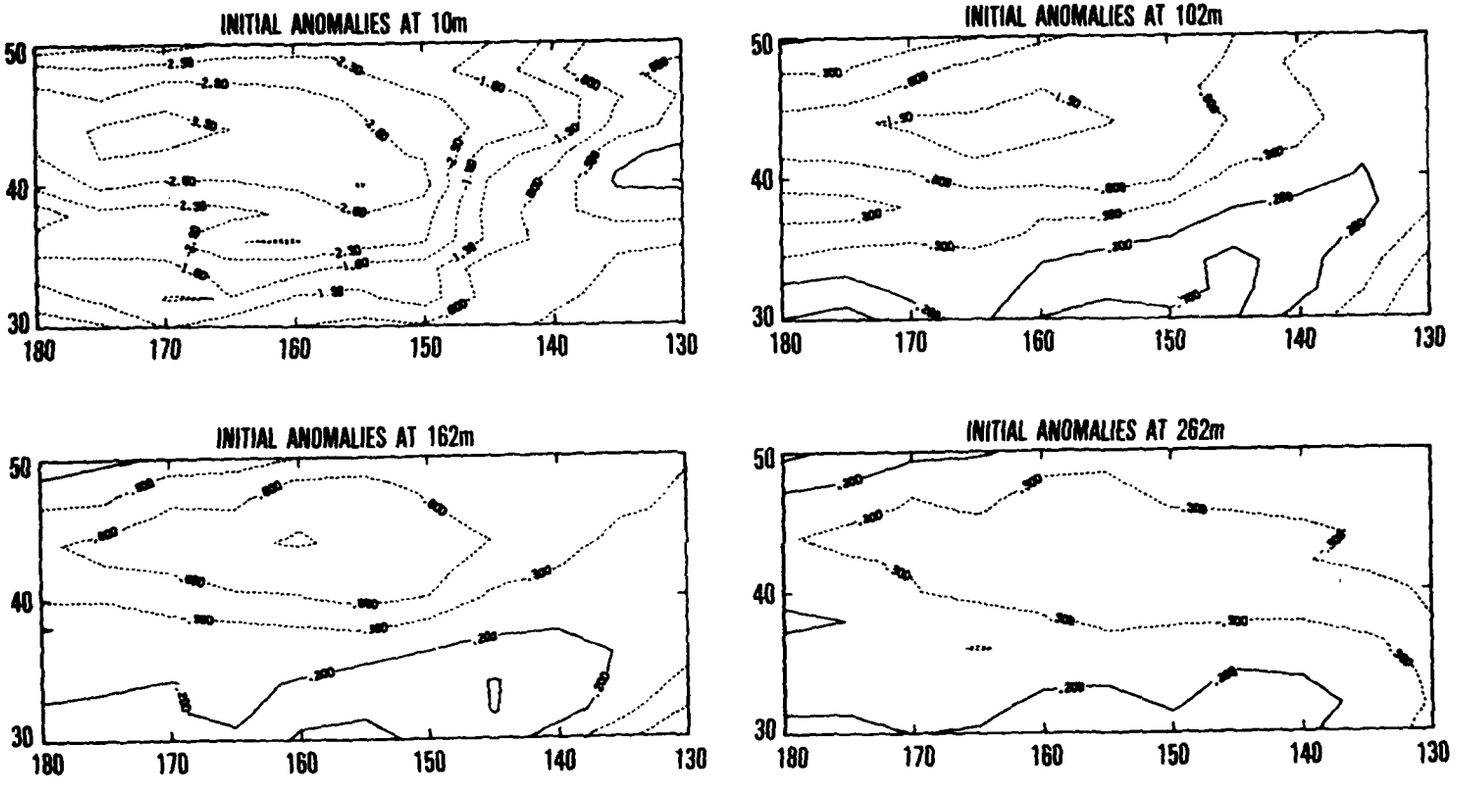

Figure 9. Initial anomalies, in °C, calculated from the OTS analysis.

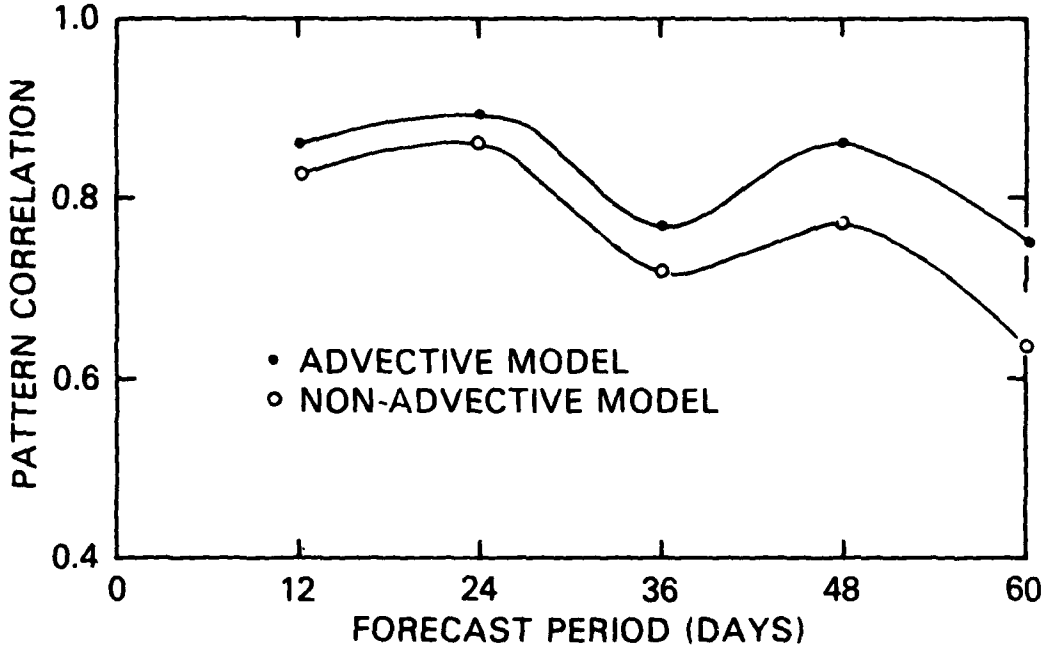

Figure 10. Pattern correlation between predicted SST anomalies and anomalies calculated from the OTS analysis for the TRANSPAC region.

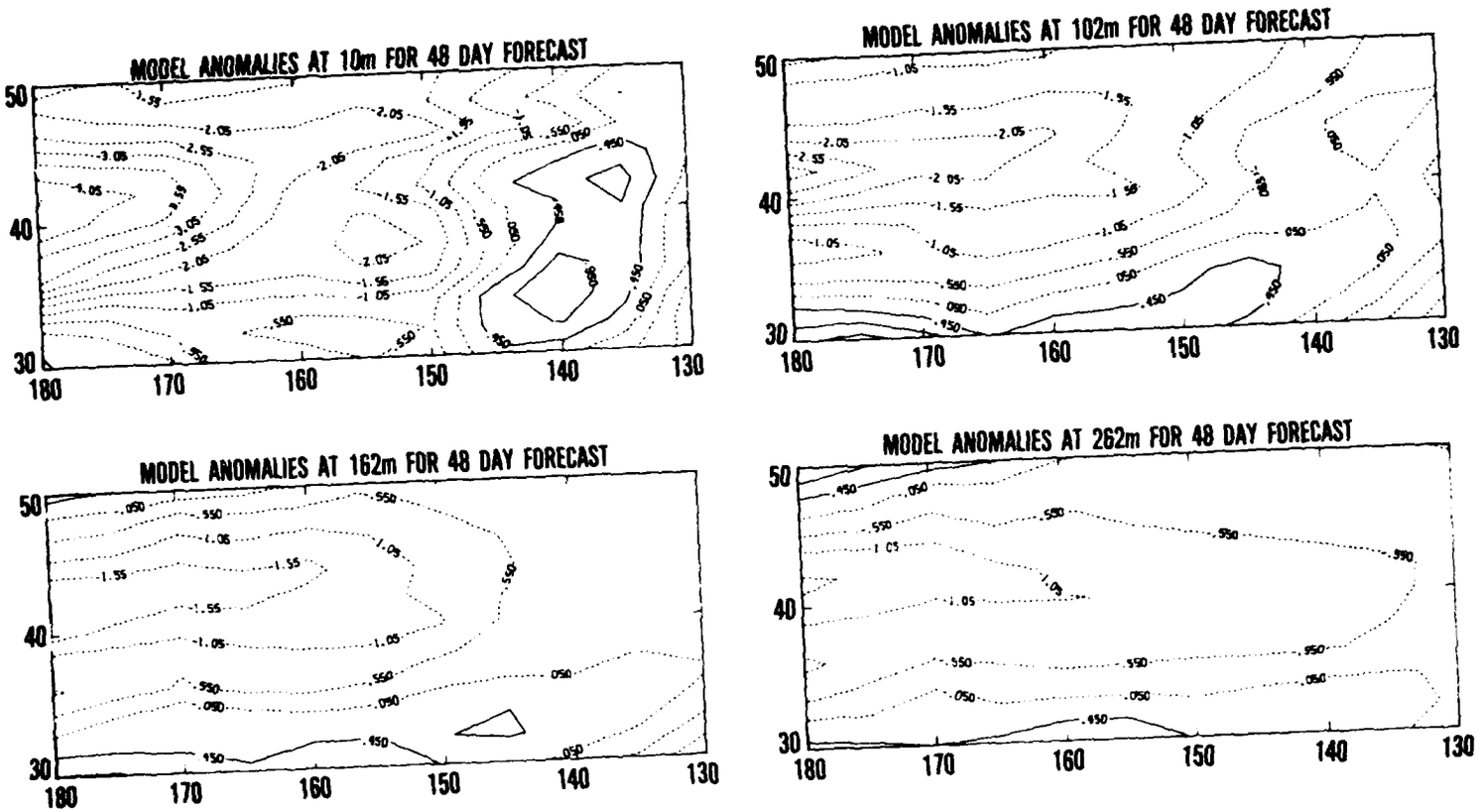

Figure 11. Anomalies predicted at Day 48 by the model with wind-drift advection. The contour interval is 0.5°C.

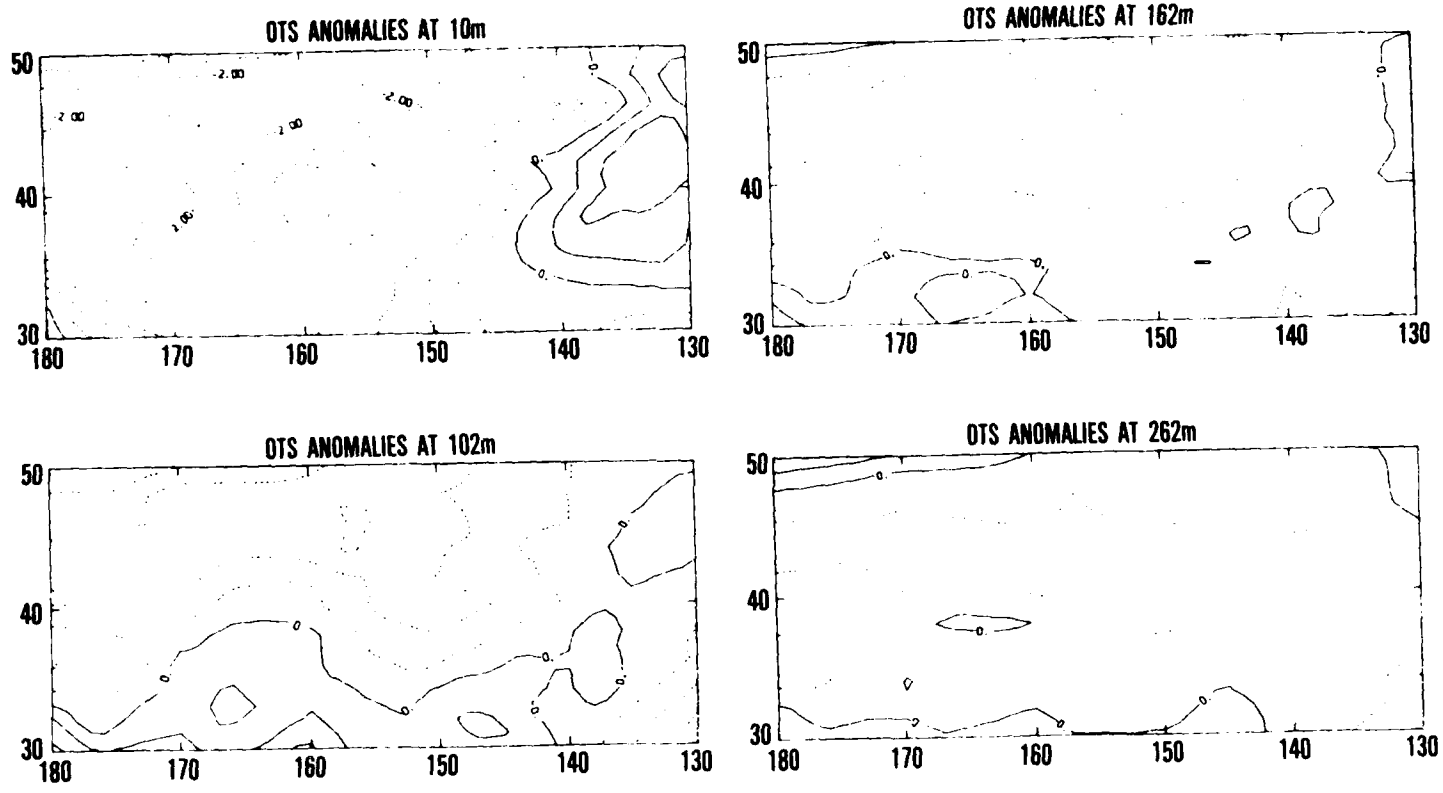

Figure 12. Anomalies calculated at Day 48 from the OTS analysis. The contour interval is 0.5°C.

anomalies are well predicted. The correlations show, on the average, a decrease in time. This suggests that the model simulations slowly diverge from the OTS analysis in time.

The anomalies predicted by the model with wind-drift advection, are shown in Figure 11. The corresponding OTS analysis anomalies are shown in Figure 12. The model simulation and the OTS analysis show the development of a cold anomaly in the upper layers of the western two-thirds of the region and a warm anomaly in the eastern third of the region. At 162 m and 262 m, there is a cold and a warm anomaly with some resemblance to the NORPAX analysis and Haney's (1980) simulation. At a depth of 262 m, the NORPAX analysis shows a widespread but weak warm anomaly.

At the depths below the mixed layer region, the patterns of the anomalies closely resemble the initial anomaly patterns. The model changes at these depths can be caused only by Ekman pumping or background eddy diffusion. The ambient diffusion has a characteristic time scale of about 30 years over 100 m. Ekman pumping can produce maximum displacements of order 10 m in 60 days. Therefore, neither of these mechanisms can make an appreciable contribution to the anomalies at the deeper depths, as evidenced by the results.

The previous analysis suggested that the model-simulated anomalies at the deeper depths are strongly dependent on the initial conditions from which the simulation is started. We studied the dependence of the anomalies on initial conditions by initializing the model from the monthly averaged NORPAX analysis instead of the OTS analysis. The results of the model simulation with wind-drift advection and an ambient viscosity of 1 cm^2/sec (i.e., ten times larger than usual) are shown in Figure 13. The anomaly in the upper layers is weaker than its analogue shown in Figure 11. At the lower depths there is a dominant warm anomaly. The trend of a cold anomaly in the surface layers and a warm anomaly at depth agrees with the NORPAX analysis.

We have also performed numerical simulations of anomalies with and without advection. As shown in Figure 10, the anomalies obtained with the model with wind-drift advection show a higher correlation with the anomalies calculated from the OTS analysis than do those predicted by the non-advective model. An analysis of the anomalies with and without advection at depths of 2.5 m, 10 m, and 50 m shows that the simulation with advection leads to colder anomalies in the western two-thirds of the region. This agrees with Haney's (1980) observation that anomalous horizontal advection produces a widespread pattern of cooling in the upper layers and plays no significant role in the deeper layers. The anomalous surface current consists of a strong Ekman flow from the north in the western two-thirds of the region. This contributes to the cold anomaly formation by horizontal advection of the colder mean temperature from the north. In the eastern third of the region the anomalous horizontal advection is weak and directed from the south (Haney, 1980).

D. STATISTICAL STUDIES

We have varied the initial conditions of the model simulations and studied the time evolution of the resulting solutions. To derive a spectrum of initial conditions, we considered the content of the OTS analysis over a 14-day interval. We chose various members of this 14-day interval for initial conditions, and we also computed a 14-day average of the OTS analysis and a standard deviation. The averaged OTS analysis and the standard deviation are shown in Figure 14. Note that the standard deviation does not exceed 1°C.

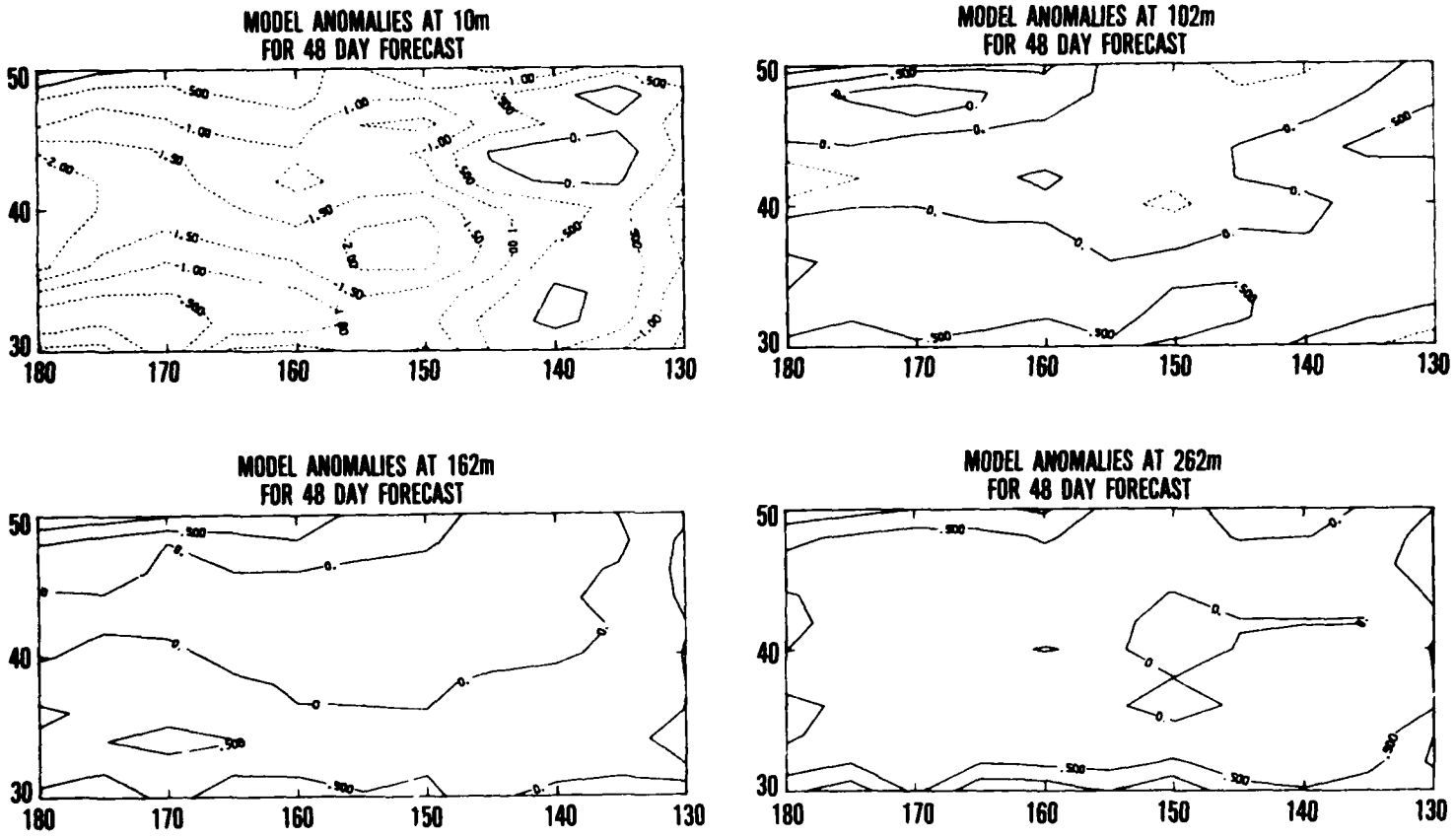

Figure 13. Same as Figure 11, but initialized from the monthly averaged NORPAX analysis instead of the OTS analysis.

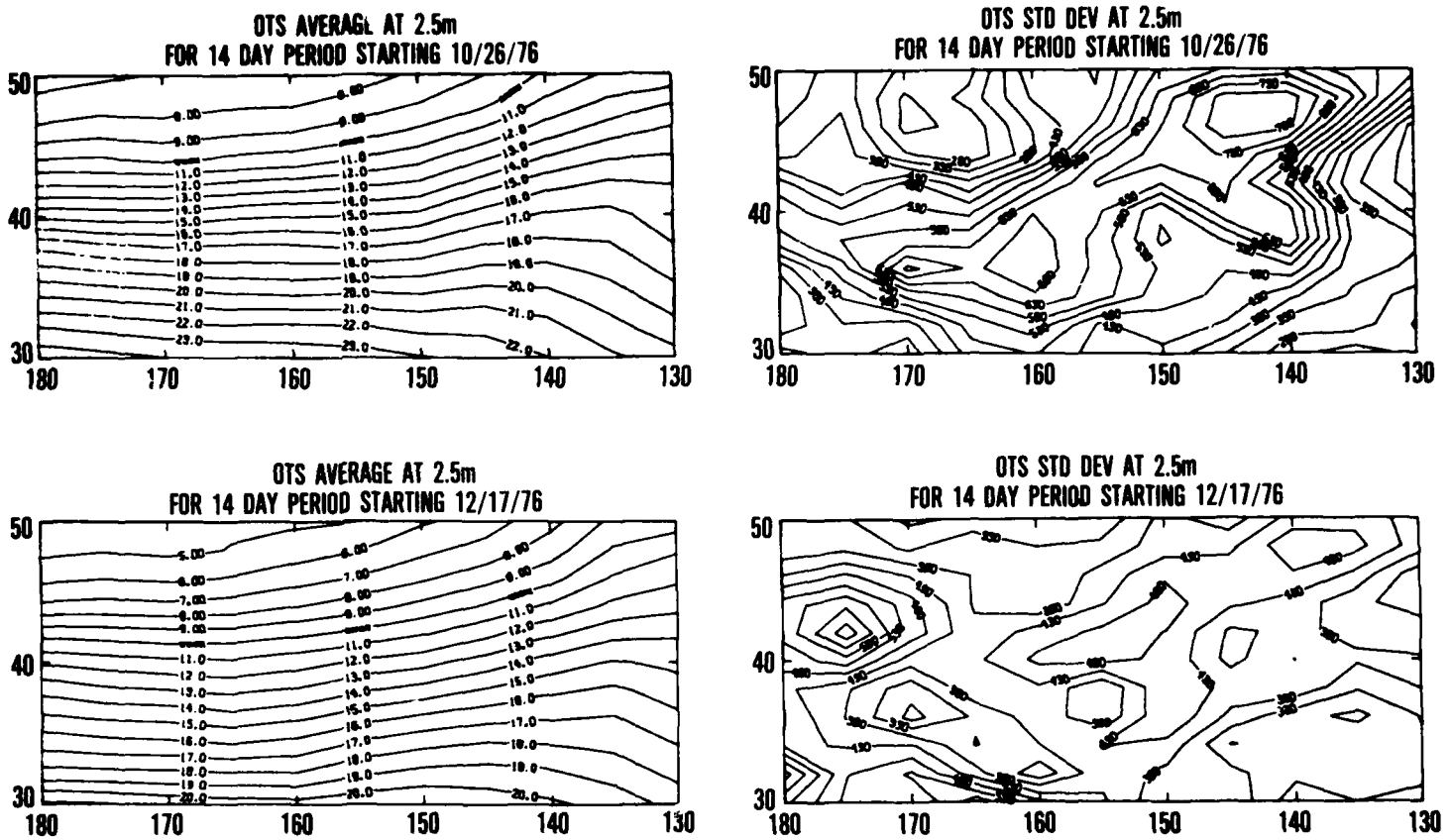

Figure 14. Fourteen-day time averages of the OTS analysis and the associated standard deviations. Units are °C.

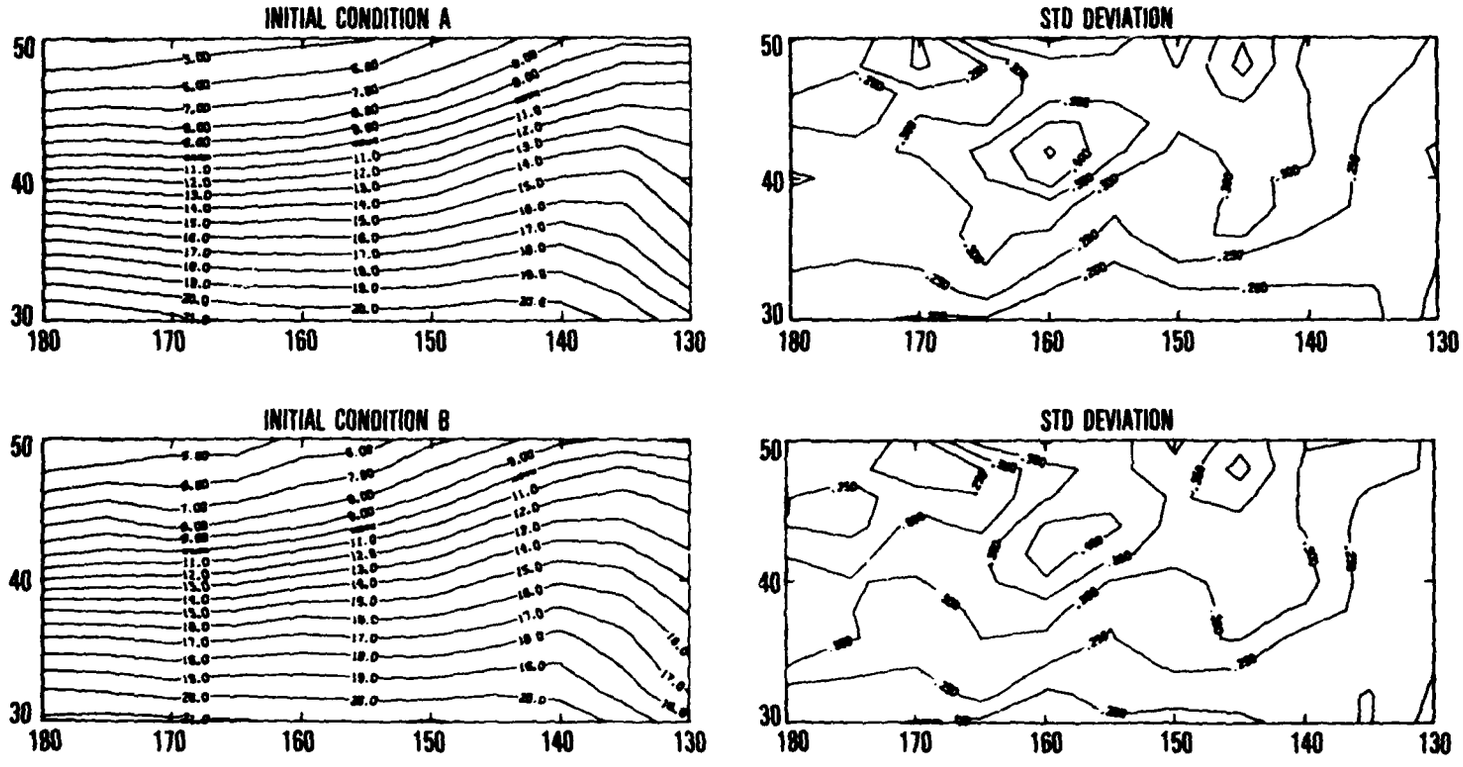

Figure 15. Twelve-day time averages and standard deviations of model solutions obtained with different initial conditions. Initial conditions chosen from an analysis of a 14-day period at the start of simulation. Units are °C.

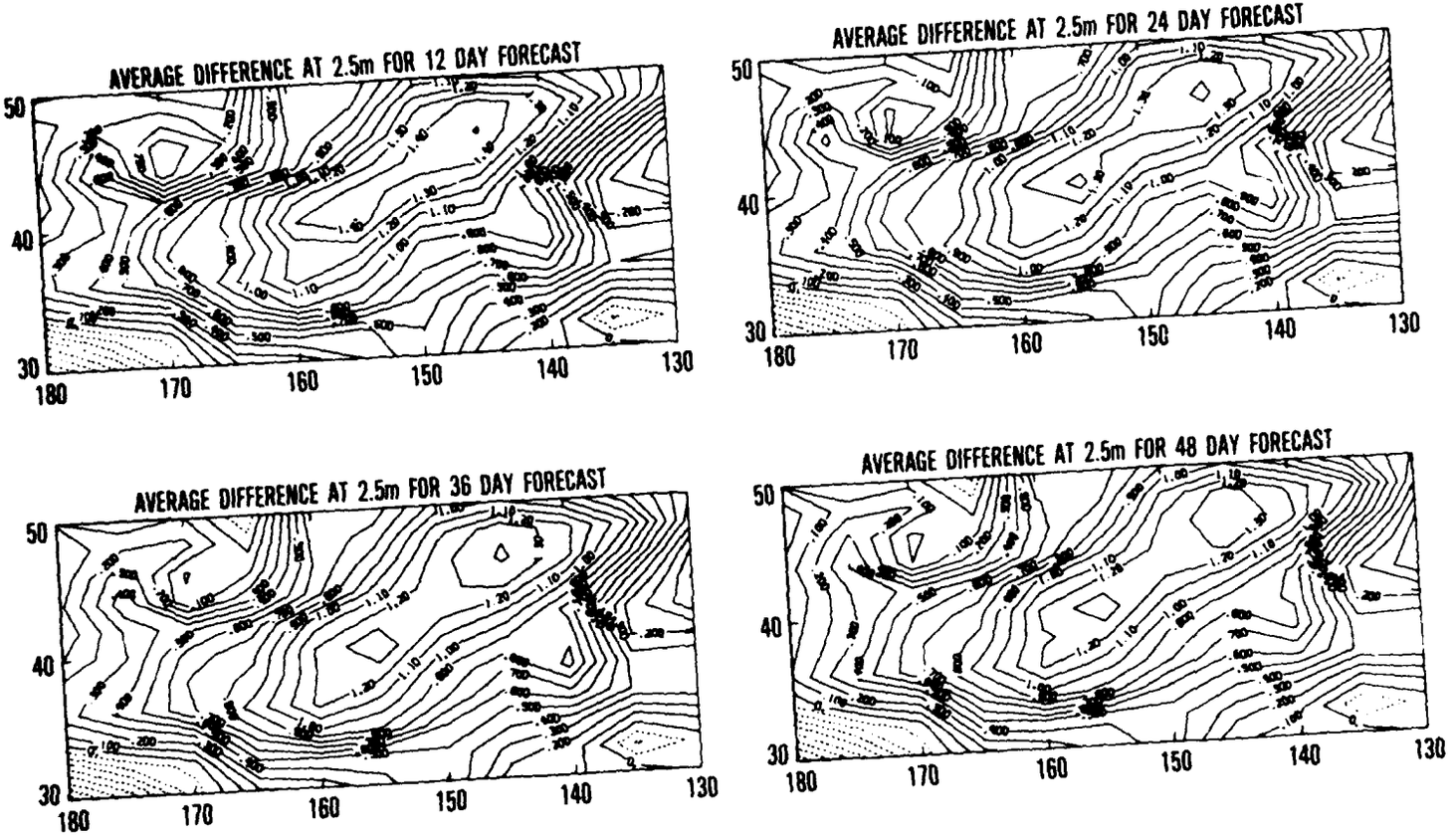

Figure 16a. Differences between two simulations started from different initial conditions. Each solution is averaged over the 12 days surrounding the indicated time of forecast. Units are °C.

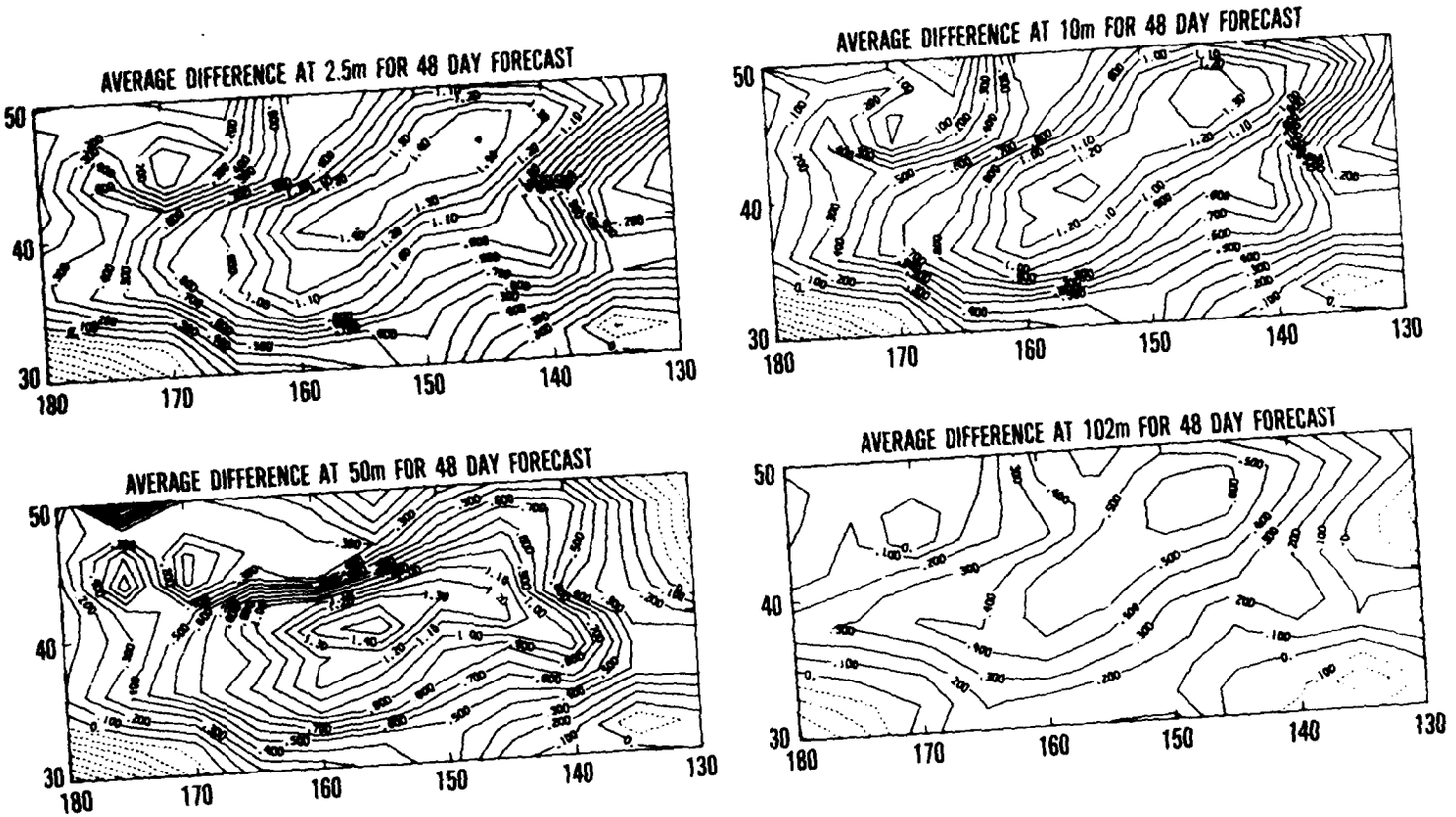

Figure 16b. Differences between two simulations started from different initial conditions. Each solution is averaged over the 12 days surrounding the indicated time of forecast. Units are °C.

In Figure 15 we show 12-day averages and standard deviations of the advective model solution at 48 days obtained from two different initial conditions. Initial condition A is the 14-day average. Initial condition B is the OTS analysis at 0000 GMT 26 October 1976. The 2.5 m isotherms at 48 days are similar in shape, with some shift in spatial location. The patterns and magnitudes of the standard deviation show close correlation.

The differences in time and space between two solutions are shown in Figure 16. One solution is initialized from an average initial condition and the other from an average plus two standard deviations. Each of the solutions is averaged over the 12 days surrounding the indicated time of forecast. The difference between solutions has a high degree of correlation in magnitude and shape. At 48 days the difference patterns correlate as a function of depth in the upper layers and decrease in correlation as the bottom of the mixed layer is approached.

The predominant signature of the differences between the solutions is the propagation of approximately the same difference patterns in time at all depths. This situation occurs because this is an externally forced problem with the evolution of the model prediction controlled by the atmospheric forcing. The problem is approximately linear in relation to the forcing, and the differences between two initial conditions propagate in time in response to it. This situation can be contrasted with the internally forced meteorological forecast problem in which small perturbations to the initial state will grow.

We have also studied the effects of phase shifts in the atmospheric forcing. We shifted the reference of the atmospheric forcing three days forward and used the model with wind-drift advection. The synoptic situation at the initial time is shown in Figure 17. There is a low pressure system, with associated warm and cold fronts, in the northern central part of the TRANSPAC region. The resulting temperature differences between the solutions arising from the variation in surface forcing are shown in Figure 18. We see the gradual development of a temperature difference of the order of 3°C at 50 m in the northwest corner of the region. The other temperature differences range up to 0.25°C in the surface layers at 60 days.

We plotted the temperature and salinity distribution versus depth for one of the points located in a large difference region. The results are shown in Figure 19. Note the presence of a temperature inversion near the bottom of the mixed layer and a corresponding increase in salinity that yields a stable density stratification. The variation in mixed-layer depth evident in Figure 19, caused by the phase shift in the atmospheric forcing, produced the large difference contours shown in Figure 18.

IV. CONCLUSION

We performed model simulations in the framework of the operational approach to ocean forecasting. Variations of the NORDA TOPS model were used to predict the future state of the ocean. The models were initialized from the OTS analysis and forced by corrected versions of the FNOC atmospheric fluxes. The predictability of the models was studied by comparing the simulations against the OTS and NORPAX analyses, and previous work.

We found that the model with wind-drift advection agreed better with the OTS analysis than the model without advection. Relative to persistence, the advective model had skill to forecast the temperature change for the TRANSPAC area over a period of 60 days. The advective model's RMS error at 60 days was approximately a

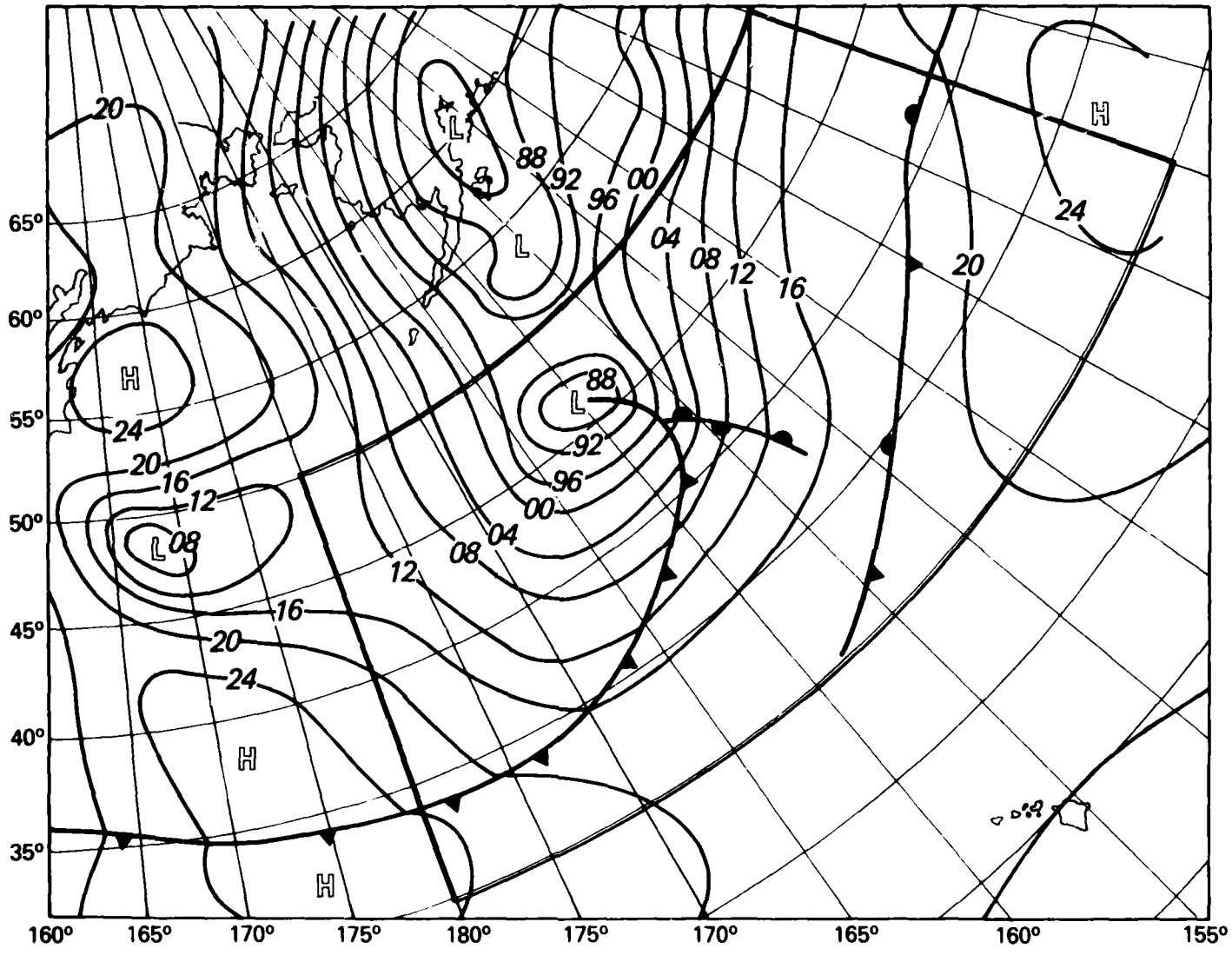

Figure 17. Surface atmospheric pressure in the TRANSPAC region at the initial time of a simulation in which the forcing is shifted three days forward. The contour interval is 4 mb and the low in the center of the region has a surface pressure of 988 mb.

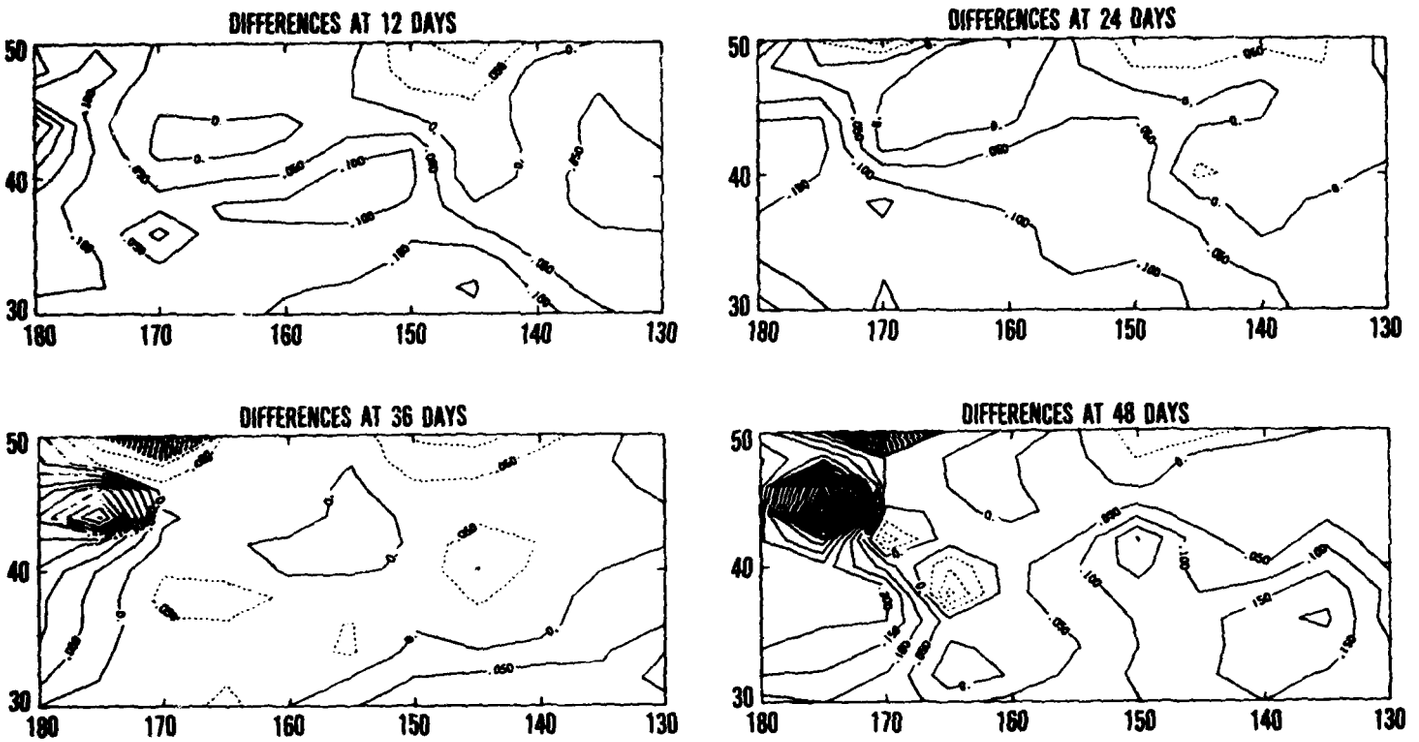

Figure 18. Difference between two solutions obtained with different atmospheric forcing and the same initial conditions. The depth is 50 m and the contour interval is 0.5°C.

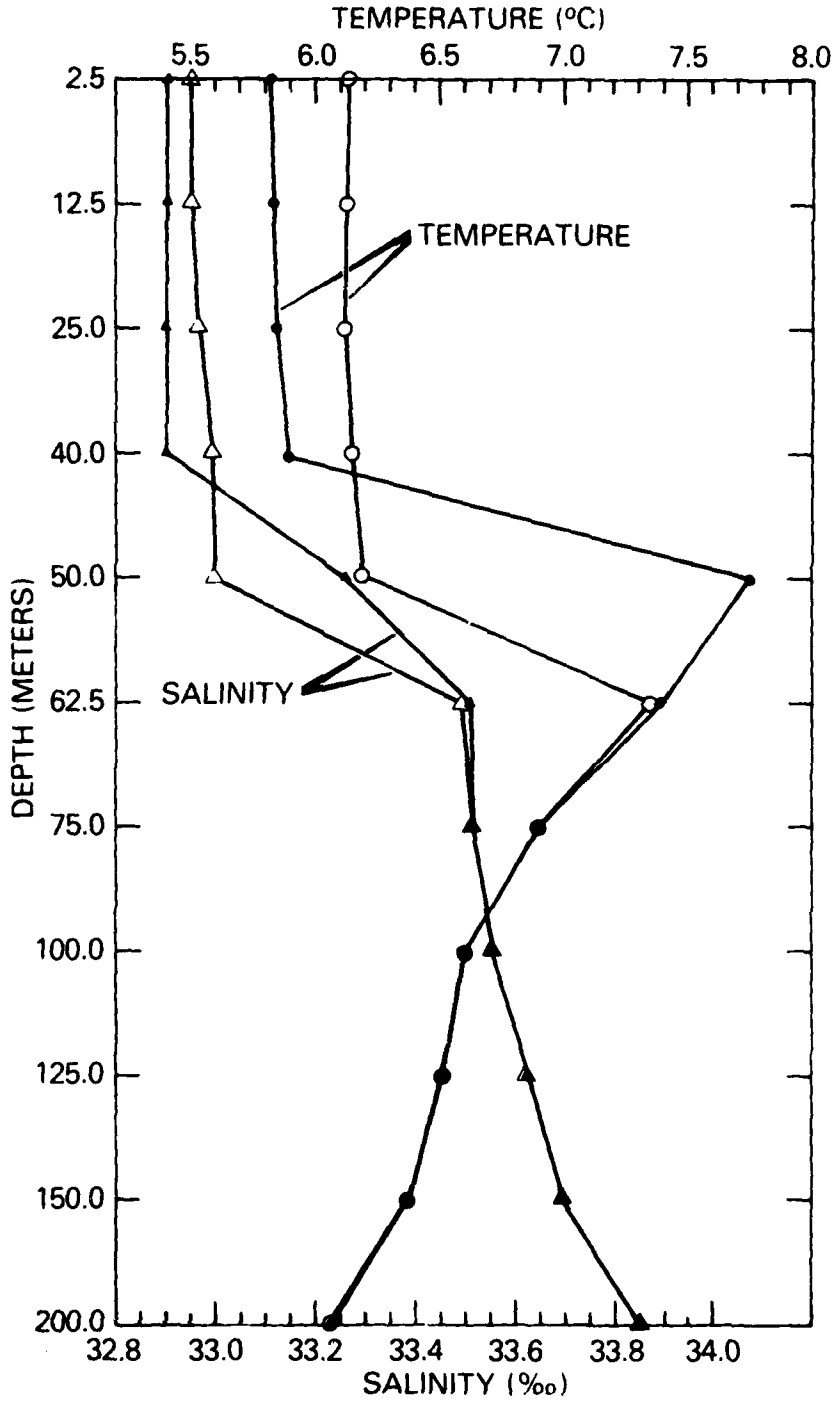

Figure 19. Temperature and salinity profiles for the area of large difference in solutions shown in Figure 18. The open symbols represent the reference solution. The solid symbols represent the solution with different atmospheric forcing.

quarter of the persistence error. This suggested that the model could be used to provide upper-ocean thermal information for regions where the ocean thermal data is sparse.

Comparisons of the OTS analysis with the monthly averaged NORPAX analysis showed differences of $\pm 1°C$. This suggested that the accuracy of the OTS analysis was of the order of the RMS forecast errors that we found when the OTS analysis was used for verification.

Our heat content and anomaly calculations indicated, in agreement with previous investigators (Barnett, 1981, and Haney, 1980), that atmospheric forcing with some form of vertical mixing controls most of the heat budget of the upper ocean. Horizontal currents tended to advect the colder northern temperatures in the upper layers of the western two-thirds of the TRANSPAC region southward. The resultant upper layer anomalies showed a cooling in the western two-thirds of the region and a warming in the eastern third, in agreement with data. At greater depths the changes in the model-simulated anomalies were very small, as evidenced by initializing the simulation with the OTS analysis and the monthly averaged NORPAX analysis.

In our statistical studies we varied the initial conditions and the atmospheric forcing. The predominant signature of the difference between solutions due to different initial conditions was the propagation of roughly the same difference pattern in time at all depths. This is because we were dealing with an approximately linear, externally forced problem, where the forcing was given by the atmospheric flux.

Short-term variations in atmospheric forcing yielded a range of temperature differences. The highest differences, up to 3°C, were produced by variation of mixed-layer depth in a region of strong temperature inversion. However, in other areas the maximum temperature differences achieved in the surface layers after 60 days were typically only about 0.25°C.

REFERENCES

Barnett, T. P. (1981). On the Nature of Large-Scale Thermal Variability in the Central North Pacific Ocean. J. Phys. Oceanogr., 11, 887-906.

Budd, B. W. (1980). Prediction of the Spring Transition and Related Sea-Surface Temperature Anomalies. Master's Thesis. Naval Postgraduate School, Monterey, Calif., 95 p.

Camp, N.T. and R. L. Elsberry (1978). Oceanic Thermal Response to Strong Atmospheric Forcing II. The Role of One-Dimensional Processes. J. Phys. Oceanogr., 8, 215-224.

Clancy, R. M. and K. D. Pollak (1982). A Real-Time Synoptic Ocean Thermal Analysis/Forecast System (in preparation).

Clancy, R. M. (1981). A Note on Finite Differencing of the Advection-Diffusion Equation. Mon. Wea. Rev., 109, 1807-1809.

Clancy, R. M. and P. J. Martin (1981). Synoptic Forecasting of the Oceanic Mixed Layer Using the Navy's Operational Environmental Data Base: Present Capabilities and Future Applications. Bull. Am. Meteorol. Soc., 62, 770-784.

Clancy, R. M., P. J. Martin, S. A. Piacsek, and K. D. Pollak (1981). Test and Evaluation of an Operationally Capable Synoptic Upper-Ocean Forecast System. NORDA Tech. Note 92, Naval Ocean Research and Development Activity, NSTL Station, MS 39529, 66 p.

Clark, N. (1972). Specification of Sea-Surface Temperature Anomaly Patterns in the Eastern North Pacific. J. Phys. Oceanogr., 2, 391-404.

Elsberry, R. L., P. C. Gallacher and R. W. Garwood (1979). One-Dimensional Model Predictions of Ocean Temperature Anomalies During Fall 1976. Tech. Rept. NPS 63-79-003, Naval Postgraduate School, Monterey, Calif., 30 p.

Haney, R. L. (1980). A Numerical Case Study of the Development of Large-Scale Thermal Anomalies in the Central North Pacific Ocean. J. Phys. Oceanogr., 10, 541-556.

Haney, R. L., W. S. Shiver and K. H. Hunt (1978). A Dynamical-Numerical Study of the Formation and Evolution of Large-Scale Ocean Anomalies. J. Phys. Oceanogr., 8, 952-969.

Haney, R. L. (1974). A Numerical Study of the Response of an Idealized Ocean to Large-Scale Surface Heat and Momentum Flux. J. Phys. Oceanogr., 4, 145-167.

Holl, M. M., M. J. Cuming, and B. R. Mendenhall (1979). The Expanded Ocean Thermal Structure Analysis System: A Development Based on the Fields by Information Blending Methodology. Tech. Rept. M-241, Meteorology International, Inc., Monterey, Calif., 216 p.

Holl, M. M. and B. R. Mendenhall (1971). Fields by Information Blending, Sea-level Pressure Version. Tech Rept. M-167. Meteorology International, Inc., Monterey, Calif., 71 p.

Jerlov, N. G. (1968). Optical Oceanography. Elsevier, N. Y., 352 p.

Kesel, P. G. and F. J. Winninghoff (1972). The Fleet Numerical Weather Central Operational Primitive-Equation Model. Mon. Wea. Rev., 100, 360-373.

Mellor, G. L. and P. A. Durbin (1975). The Structure and Dynamics of the Ocean Surface Mixed Layer. J. Phys. Oceanogr., 5, 718-725.

Mellor, G. L. and T. Yamada (1974). A Hierarchy of Turbulence Closure Models for Planetary Boundary Layers. J. Atmos. Sci., 31, 1791-1806.

Mendenhall, B. R., M. J. Cuming and M. M. Holl (1978). The Expanded Ocean Thermal-Structure Analysis System Users Manual. Tech. Rept. M-232, Meteorology International, Inc., Monterey, Calif., 110 p.

Mihok, W. F. and J. E. Kaitala (1976). U.S. Navy Fleet Numerical Weather Central Operational Five-Level Global Fourth-Order Primitive-Equation Model. Mon. Wea. Rev., 104, 1527-1550.

Niiler, P. P. and E. B. Kraus (1977). One-Dimensional Models of the Upper Ocean. In Modelling and Prediction of the Upper Layers of the Ocean, edited by E. B. Kraus, Pergamon, N. Y., Chapt. 10, pp. 143-172.

Pollard, R. T., P. B. Rhines and R. O. Thompson (1973). The Deepening of the Wind Mixed Layer. Geophys. Fluid Dyn., 3, 381-404.

Pollard, R. T. and R. C. Millard (1970). Comparison Between Observed and Simulated Wind-Generated Inertial Oscillations. Deep Sea Res., 17, 813-821.

Thompson, R. O. (1976). Climatological Numerical Models of the Surface Mixed Layer of the Ocean. J. Phys. Oceanogr., 6, 496-503.

Weigle, W. R. and B. R. Mendenhall (1974). Climatology of the Upper Thermal Structure of the Seas. Tech. Rept., M-196, Meteorology International, Inc., Monterey, Calif., 79 p.

White, W. B. and R. L. Bernstein (1979). Design of an Oceanographic Network in the Midlatitude North Pacific. J. Phys. Oceanog., 9, 592-606.

UNCLASSIFIED

SECURITY CLASSIFICATION OF THIS PAGE *(When Data Entered)*

REPORT DOCUMENTATION PAGE	READ INSTRUCTIONS BEFORE COMPLETING FORM
1. REPORT NUMBER: NORDA Technical Note 156	2. GOVT ACCESSION NO.: AD-A118 159
3. RECIPIENT'S CATALOG NUMBER	
4. TITLE *(and Subtitle)*: Studies of Large-Scale Thermal Variability with a Synoptic Mixed-Layer Model	5. TYPE OF REPORT & PERIOD COVERED: Final
6. PERFORMING ORG. REPORT NUMBER	
7. AUTHOR(s): A. Warn-Varnas, M. Clancy, M. Morris, P. Martin, S. Horton	8. CONTRACT OR GRANT NUMBER(s)
9. PERFORMING ORGANIZATION NAME AND ADDRESS: Naval Ocean Research & Development Activity, Ocean Science & Technology Laboratories, Code 322, NSTL Station, Mississippi 39529	10. PROGRAM ELEMENT, PROJECT, TASK AREA & WORK UNIT NUMBERS
11. CONTROLLING OFFICE NAME AND ADDRESS: Naval Ocean Research & Development Activity, Ocean Science & Technology Laboratories, Code 322, NSTL Station, Mississippi 39529	12. REPORT DATE: June 1982 13. NUMBER OF PAGES: 38
14. MONITORING AGENCY NAME & ADDRESS *(if different from Controlling Office)*	15. SECURITY CLASS. *(of this report)* 15a. DECLASSIFICATION/DOWNGRADING SCHEDULE

16. DISTRIBUTION STATEMENT *(of this Report)*

Approved for Public Release
Distribution Unlimited

17. DISTRIBUTION STATEMENT *(of the abstract entered in Block 20, if different from Report)*

18. SUPPLEMENTARY NOTES

19. KEY WORDS *(Continue on reverse side if necessary and identify by block number)*

Ocean Analysis	Oceanic Mixed Layer
Ocean Prediction	Ocean Circulation
Ocean Forecast Model	NORPAX
Ocean Thermal Structure	TRANSPAC

20. ABSTRACT *(Continue on reverse side if necessary and identify by block number)*

This work was performed to investigate a number of aspects of operational ocean forecasting including model initialization and forcing, physical parameterizations, and the importance of various processes that modify upper-ocean thermal structure. A synoptic mixed-layer model was used to perform numerical simulations in the TRANSPAC region of the Central North Pacific. The multilevel model incorporates the Mellor and Yamada (1974) Level-2 turbulence parameterization and advection by wind-drift currents.

DD FORM 1 JAN 73 1473 EDITION OF 1 NOV 65 IS OBSOLETE
S/N 0102-LF-014-6601

UNCLASSIFIED

SECURITY CLASSIFICATION OF THIS PAGE *(When Data Entered)*

The model was initialized and forced by fields produced operationally at the U.S. Navy's Fleet Numerical Oceanography Center. Initialization was from the FNOC Ocean Thermal Structure (OTS) analysis and forcing was by surface wind and flux fields associated with the FNOC Northern Hemisphere Primitive Equation and Planetary Boundary Layer Models.

We performed a 60-day simulation of the time span from November to December 1976. Simulations were conducted both with and without wind-drift advection. The results were compared with the daily FNOC OTS analysis, the monthly TRANSPAC XBT analysis, the anomaly calculations of Haney (1980), and forecasts of persistence and climatology.

A comparison of model-predicted sea surface temperature with the OTS analysis showed that the model gave a consistently better forecast than persistence or climatology. Dropping advection from the model decreased its skill. A similar conclusion prevailed when we compared pattern correlations of the predicted and analyzed changes from the initial state.

A comparison of model-simulated changes in upper-ocean heat content with the OTS analysis showed a bias in the FNOC net surface heat flux. The bias was confirmed by a comparison with the flux calculations of Nate Clark. The cause of this bias was most likely excessive latent heat loss.

In the mixed-layer region, the model-simulated anomalies showed a cooling trend in the western two-thirds of the TRANSPAC region and a warming trend in the eastern one-third. This trend agreed with observations. The inclusion of advection improved the agreement.

Variations in initial conditions and analysis of the differences in subsequent solutions showed a propagation of the same difference pattern in time in the mixed-layer region. This confirms that upper-ocean variability is dominated by external forcing.


FILMED
9-8